AD NUMBER

AD882641

NEW LIMITATION CHANGE

TO

Approved for public release, distribution unlimited

FROM

Distribution authorized to U.S. Gov't. agencies only; Test and Evaluation; Apr 1971. Other requests shall be referred to Commander, Naval Air Systems Command, Attn: Air-310B, Washington, dc 20360.

AUTHORITY

USANASC ltr, 1 Sep 1973

(2)

Contract N00019-70-C-0397

INTEGRATED CONFORMAL ARRAYS

FINAL REPORT

MARCH 1970 TO JANUARY 1971

Prepared for the AIR SYSTEMS COMMAND
Department of the NAVY

Creating a new world with electronics

HUGHES

ANTENNA DEPARTMENT, AEROSPACE GROUP
HUGHES AIRCRAFT COMPANY
CULVER CITY, CALIFORNIA

61

DOCUMENT TRANSMITTAL
NAVAIR FORM 3900/3 (10-67)

CLASSIFICATION: UNCLASSIFIED

UNCLASSIFIED WHEN ENCLOSURE IS REMOVED

SERIAL NUMBER (When required)/DATE:

AD NUMBER (To be inserted by DDC):

ORIGINATING AGENCY: Hughes Aircraft Company

REPORT SERIES AND NUMBER: 2765.01/266
HAC Ref. no.C-1498

ENCLOSURE (Report title):
INTEGRATED CONFORMAL ARRAYS
Final report
(March 1970-Jan. 1971)
Limitation B
Gov-DDC
Others-AIR-310B (2 cops)

REPORT DATE: Feb. 15, 1971

COG. NAVAIR CODE: AIR-310B

CONTRACT/PROJECT/AIRTASK NUMBER: N00019-70-C-0397

TO
Administrator
Defense Documentation Center for Scientific and Technical Information (DDC)
Bldg #5, Cameron Station
Alexandria, Virginia 22314

SECURITY CLASSIFICATION

	UNCLAS	CONFI	SECRET	RD
REPORT	X			
TITLE OR SUBJECT	X			
ABSTRACT OR SUMMARY	X			

Enclosure is forwarded for distribution subject to limitations checked below. Request AD number be inserted in space above; two copies of this letter be returned to originating activity if shown below; two copies be sent to Commander, Naval Air Systems Command; and one copy be retained by DDC.

☐ 1. This document has been approved for public release and sale. Its distribution is unlimited.

IN ADDITION TO SECURITY REQUIREMENTS WHICH APPLY TO THIS DOCUMENT AND MUST BE MET -

☐ 2. This document is subject to special export controls and each transmittal to foreign governments or foreign nationals may be made only with the prior approval of

☐ 3. Each transmittal of this document outside the agencies of the U. S. Government must have prior approval of

☐ 4. Each transmittal of this document outside the Department of Defense must have prior approval of

☐ 5. This document may be further distributed by the holder only with specific prior approval of

DISTRIBUTION STATEMENT: B Test and evaluation April 1971

SIGNATURE: (Mrs.) Julia M. Lutz

TITLE: Julia M. Lutz
By direction

CODE: AIR-604A

DATE: 4-19-71

CLASSIFICATION: UNCLASSIFIED

Commander Naval Air Systems Command (AIR-604)
Navy Department
Washington, D. C. 20360

S/N-0102-603-3910

UNCLASSIFIED WHEN ENCLOSURE IS REMOVED

GPO 872-405 C-17

Report No. 2765.01/266
HAC Ref. No. C-1498

INTEGRATED CONFORMAL ARRAYS

CONTRACT N00019-70-C-0397

FINAL REPORT

March 1970 to January 1971

Prepared by

W. H. Kummer
M. C. Behnke
A. F. Seaton
A. T. Villeneuve

Prepared for

Air Systems Command
Department of the Navy
Washington, D. C.

Microwave Radar Laboratory
Radar Division
AEROSPACE GROUP

Hughes Aircraft Company - Culver City, California

ACKNOWLEDGMENTS

The following personnel of the Hughes Radar Division contributed to the Integrated Conformal Array Program during this period:

Dr. W. H. Kummer	Program Manager Radar Microwave Laboratory
M. C. Behnke	Antenna Department
Dr. T. S. Fong	Radar & Signal Processing Laboratory
L. M. Frederick	Antenna Department
A. F. Seaton	Antenna Department
Dr. A. T. Villeneuve	Antenna Department

The Technical Officer for this program is Mr. J. W. Willis (AIR-310B).

ABSTRACT

Two distinct aspects were investigated in this program. The first one is concerned with the synthesis of far field patterns from sources on the conical surface. Three different approaches were undertaken:

(1) An equivalence principle was used to determine the distribution of sources on a cone to produce a prescribed pattern in the far field.

(2) Roots of two transcendental equations were calculated for appropriate parameters. The numerical values are needed for a theoretical solution of the radiation fields and mutual coupling effects in a region bounded by a conducting cone.

(3) Computation of patterns from discrete radiators placed on a conical surface was continued. The signal-to-noise ratio is optimized in the beam pointing direction.

The second aspect included the design, fabrication and testing the scanning capabilities of a linear array of crossed slots on a large ground plane. The array was designed so that each radiating element could be matched in the presence of the others, its phase and amplitude could be arbitrarily set and the active impedance measured. The array scanned from broadside to 80° (10° from endfire) with satisfactory beam patterns and sidelobe levels.

CONTENTS

LIST OF ILLUSTRATIONS

ILLUSTRATIONS - Continued

1.0 INTRODUCTION AND SUMMARY

A continuing study of Integrated Conformal Arrays was conducted under Contract N00019-70-C-0397 during the period March 1970 to January 1971 by personnel of the Radar Division, Hughes Aircraft Company. The program has as its goal the development of an electronically steered conformal array integral with the surface of a slender cone. For purposes of this program, a cone angle of 20° was selected; the frequency was chosen at X-band. It is felt that a blunter cone and other frequencies would work equally well once feasibility has been demonstrated with the geometry chosen.

In this program two distinct aspects were investigated. The first one is concerned with the synthesis of far field patterns from current distributions on the conical surface. Since there are no proven techniques for synthesizing antenna patterns from arrays on conical surfaces, three different approaches to this problem have been pursued:

1. An equivalence principle was used to determine the distribution of sources on a cone to produce a prescribed pattern. Using this approach planar arrays are replaced by sources on a conformal surface. Thus, it is possible to generate patterns using well known synthesis techniques for planar surfaces. The equivalent sources are continuous functions on the cone. The practical validity of the method depends on the accuracy with which the continuous functions can be approximated by physically realizable radiators.

2. The roots of two transcendental equations involving the associated Lengendre functions and their derivatives were calculated numerically. The calculations make available the required tools for exact theoretical solutions of the radiation fields and mutual coupling effects in a region bounded by a conducting cone.

3. The computation of patterns from discrete radiators judiciously positioned on the cone was continued. An optimization is performed to obtain the highest signal-to-noise ratio in the beam pointing direction. The sidelobes resulting from this method have asymmetrical distributions with high values in some regions.

A linear array of crossed slots located in a ground plane was designed, fabricated and tested to scan over wide angles. The array was designed so that each radiating element could be matched in the presence of the others; the phase and amplitude radiated from each could be set as desired. The array included provisions for the measurement of the active impedance of each radiating element.

Two initial conditions were set up. The array was matched at broadside and at 80°. Continuous scan was obtained from broadside to 80° for both conditions. The beam pointing direction was close to that calculated theoretically; the sidelobe levels were satisfactory. Beyond 80° the beam position did not change. Thus scanning to within 10° of endfire is practical for a linear array on an infinite ground plane.

2.0 PATTERN SYNTHESIS

An equivalence principle was applied to the problem of determining the distribution of sources on a cone to produce a prescribed pattern. By this method, more conventional sources such as planar or linear arrays are replaced by sources on a conformal surface such as a cone. The method and patterns synthesized by it are discussed.

2.1 GENERAL APPROACH TO ANTENNA PATTERN SYNTHESIS FROM SOURCES ON A CONDUCTING SURFACE

The problem of interest is that of forming various steerable antenna patterns by distributing sources over the surface of a vehicle. The patterns that are desirable are essentially those that would be obtained from a circular or an elliptical planar aperture. The beam would be steered electronically.

The initial problem is to produce the pattern of a conventional antenna such as is illustrated in Figure 2-1, by sources on an aerodynamic surface.

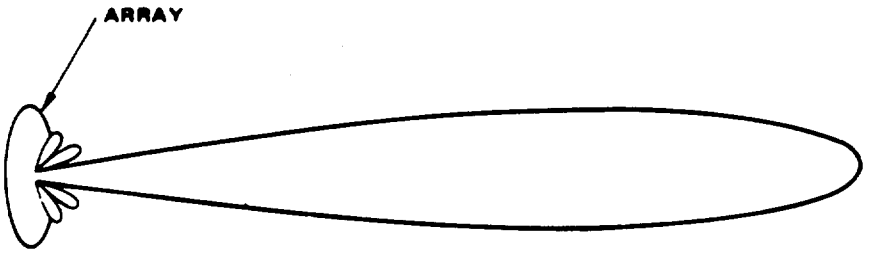

Figure 2-1. Array with conventional pattern

If the proper equivalent magnetic source currents can be synthesized on the conducting surface, the original field will result at all points exterior to the surface. In the case of interest, the original source is a planar array and the metal surface is a conical or ogival

surface. The magnetic current sheets are surface distributions of magnetic dipoles. A magnetic dipole can be approximated by slots on a conducting surface. By proper orientiation and excitation of slots on the metallic surface, the desired exterior field can the be approximated. The required source distribution is known exactly since the initial fields are known.

The antenna utilized in determing the sources on a cone that are equivalent to a planar array is a circular planar array of parallel slots that may be oriented arbitrarily within the conical surface. Its pivotal point is located far enough from the cone apex to permit motion of the array without intersecting the conical surface.

The positioning of the equivalent planar array does not take advantage of the total conical surface when the beam is pointing directly through the cone tip. However, this arrangement is a relatively simple one that provides an invariant pattern as the beam direction is changed. It is possible to take advantage of the total conical surface as the beam is moved through the cone tip by making the diameter of the equivalent planar array larger. The array may be moved back along the cone axis as a function of beam position so that the equivalent planar array just fills the cone base when it is looking through the cone tip. The equivalent sources are continuous functions of position on the surface of the cone and must be approximated by discrete sources (slots) for a real antenna system. The patterns resulting from the discrete sources must be calculated and compared with the desired patterns to check the validity of the technique.

2.2 STUDY OF ELECTROMAGNETIC FIELDS OF SOURCES ON CONDUCTING CONES

More exact calculations of radiation fields and calculations of mutual coupling effects require the determination of the electromagnetic fields of sources on the surface of a conducting cone. In this section two studies are discussed. One is devoted to the exact calculation of these fields and the second is devoted to an approximate solution for the radiation fields of such sources.

Radiation from Slots on a Conducting Cone

The problem of radiation from slots on a conducting cone has been attacked and formally solved by Bailin and Silver (1956). The general solution uses the electromagnetic fields expanded in spherical functions. The functions are then matched to the appropriate boundary conditions for the particular problem to be solved. The fields are obtained from vector potential which have solutions in the exterior region to the cone of the form

$$\Pi_{\nu m} = Z_{\nu}(kr)\, P_{\nu}^{m}(\cos\theta)\left\{A_m \cos m\phi + B_m \sin m\phi\right\} \quad (2\text{-}1)$$

where $Z_{\nu}(kr)$ are Bessel functions expressing the radial dependence

$P_{\nu}^{m}(\cos\theta)$ are the associated Legendre functions with ν being non-integral.

In order to satisfy the boundary conditions the roots ν_i of the following equations must be obtained

$$P_{\nu_i}^{m}(\cos\theta_o) = 0$$

and

$$\left.\frac{\partial P_{\nu_i}^{m}(\cos\theta)}{\partial\theta}\right|_{\theta=\theta_o} = 0 \quad (2\text{-}2)$$

where $P_{\nu}^{m}(x)$ is the associated Legendre function of the first kind of order m and degree ν. The cone half-angle is $\pi - \theta_o$. Since the cone angle is small in general, a suitable representation for rapid convergence of the associated Legendre function of the zeroth order and the argument near -1 is (Gray, 1953).*

*The nomenclature for the order and degree of the Legendre functions are interchanged in Gray's paper from that used here.

$$P_\nu^o\left[\cos(\pi-\alpha)\right] = \left[2\frac{\sin\nu\pi}{\pi}\log(\sin\alpha/2) + \cos\nu\pi\right] P_\nu^o(\cos\alpha)$$

$$+ \frac{\sin\nu\pi}{\pi}\sum_{r=o}^{\infty}\frac{(-1)^r(\nu+r)!}{(\nu-r)!}$$

$$\cdot\left[\psi(\nu+r) + \psi(\nu-r) - 2\psi(r)\right]\frac{(\sin\alpha/2)^{2r}}{r!\,r!} \qquad (2\text{-}3)$$

where $\alpha = \pi - \theta_o$, the cone half-angle,

$$P_\nu^o(\cos\alpha) = \sum_{r=o}^{\infty}\frac{(-1)^r(\nu+r)!}{(\nu-r)!\,r!\,r!}(\sin\alpha/2)^{2r} \qquad (2\text{-}4)$$

and

$$\psi(\xi) = \frac{d}{d\xi}(\log\xi!). \qquad (2\text{-}5)$$

Because of the factors $(\nu+r)!$, $\psi(\nu+r)$, and $\psi(\nu-r)$ that grow rapidly with an increase in ν, the above expressions are suitable only for the computation of small ν values. Consequently, only for ν belonging in the closed interval $\left[0, 2\right]$[+] was $P_\nu^o(\cos\theta_o)$ computed by Eq. (2-3); and for higher values of ν, the following recurrence formula with m set equal to zero was used

$$P_{\nu+1}^m(x) = \frac{1}{(\nu-m+1)}\left[(2\nu+1)xP_\nu^m(x) - (\nu+m)P_{\nu-1}^m(x)\right] \qquad (2\text{-}6)$$

For a reasonable accuracy in the numerical solution of the radiation problem, the number of eigenvalues needed is approximately 70 for each order m, m = 1, 2, ... , 15, or equivalently, it suffices to determine $P_\nu^m(\cos\theta_o)$ for only $\nu \in \left[0, 80\right]$ for each m, m = 1, 2, . . . , 15. For orders, m = 1, 2, 3, . . . , 15, $P_\nu^m(\cos\theta_o)$, $\nu \in \left[0, 80\right]$ was determined by the following recurrence formula

$$P_\nu^{m+1}(x) = \frac{1}{\sqrt{1-x^2}}\left[(\nu-m)xP_\nu^m(x) - (\nu+m)P_{\nu-1}^m(x)\right] \qquad (2\text{-}7)$$

[+]The symbol $\in$ will be used to indicate "belonging to". The symbol $\left[a, b\right]$ indicates the closed interval beginning at "a" and ending at "b". Thus $\nu \in \left[0, 2\right]$ means ν belonging in the closed interval $\left[0, 2\right]$.

For $\frac{\partial}{\partial \theta} P_\nu^m(\cos \theta_o)$, $\nu \in \left[0, 80\right]$, m = 0, 1, 2, ..., 15, the following formula (together with Eq. (2-6) and Eq. (2-7) was used:

$$\frac{\partial}{\partial x} P_\nu^m(x) = \frac{1}{1-x^2}\left[(\nu - m + 1) P_{\nu+1}^m(x) - (\nu+1)x P_\nu^m(x)\right] \qquad (2\text{-}8)$$

Since these functions are evaluated only at a finite number of discrete ν values (at interval 1/64) their zero crossings or roots must be interpolated. A linear interpolation formula for this situation is adequate since the function near zero behaves nearly linearly over a small region. A summary of the computational steps is given below:

1. Compute and store $P_\nu^o(\cos \theta_o)$ for $\nu \in \left[0, 2\right]$ at $\Delta\nu = 1/64$ using Eq. (2-3).
2. Compute and store $P_\nu^o(\cos \theta_o)$ for $\nu \in \left[2, 80\right]$ at $\Delta\nu = 1/64$ using the stored values in 1 with Eq. (2-6).
3. Compute $\frac{\partial}{\partial \theta} P_\nu^o(\cos \theta_0)$ for $\nu \in \left[0, 80\right]$ by Eq. (2-8) using the stored values in 2.
4. Interpolate for the zero crossings of $P_\nu^o(\cos \theta_o)$ and $\frac{\partial}{\partial \theta} P_\nu^o(\cos \theta_0)$ for $\nu \in \left[0, 80\right]$.
5. Compute and store $P_\nu^1(\cos \theta_o)$ for $\nu \in \left[0, 80\right]$ by Eq. (2-7) using the stored values in 1 and 2.
6. Compute $\frac{\partial}{\partial \theta} P_\nu^1(\cos \theta_o)$ for $\nu \in \left[0, 80\right]$ by Eq. (2-8) using the stored values in 5.
7. Interpolate for the zero crossings of $P_\nu^1(\cos \theta_o)$ and $\frac{\partial}{\partial \theta} P_\nu^1(\cos \theta_o)$ for $\nu \in \left[0, 80\right]$.
8. Repeat steps 5 to 7 but increase the order each time and use the previously stored values to recur upward in m.

Two computer programs were written, one to compute the zeros of the function, and one to compute the zeros of the derivative of the function. A listing of the first program is given in Appendix I, and a listing of the second in Appendix II. Both programs will be used as subroutines in a main program that is to be written to compute the far-field pattern of the conformal array. A detailed discussion of the computation of antenna patterns from a conical surface was given by Villeneuve (1968). Because there is some commonality in the two programs, part of the second program can be eliminated when they are both used as subroutines to the same main program. Since a large number of recurrence operations are involved, double precision arithmetic is employed throughout the computation in order to minimize the roundoff errors. The time required to compute the eigenvalues needed for one array pattern is approximately one minute on a GE 635 computer.

2.3 PATTERN COMPUTATIONS

The program for computing patterns of the conical array (Kummer, et al, 1970) was modified so that it will handle elements arranged in a staggered configuration similar to that shown in Figure 4-10. Sixteen elements per circle were assumed for the initial computation. With that number of elements per circle, it was estimated that 10 circles of elements would fit on the cone. Thus, a total of 160 elements "filled" the large end of the cone. The small end of the cone was left "empty." A number of patterns have been computed with this program for various beam pointing directions. An examination of these patterns when scanned to the nose-fire position revealed a sizable difference in beamwidth in the two principal plane cuts. This result was unusual for the pattern from a circular aperture.

The computer program being used incorporates a weighting function which maximizes the signal-to-noise ratio of a received signal. The program weighs the signal received by each antenna element in a ratio proportional to the pattern of that element in the beam pointing direction. The program also adjusts the polarization radiated from each element so that it is linear and the same for all elements in the beam pointing direction.

It was suspected that the resulting amplitude distribution might be having an unequal effect on the beamwidth in the two patterns. The weighting function was suppressed and a uniform amplitude assumed over the whole "filled" area. Computed patterns showed that the difference in beamwidths was reduced significantly. Some differential in beamwidths did remain, however, and it was decided to complete the modification of the computer program so that the whole cone could be "filled" with elements in a staggered configuration. This has been done and some preliminary results obtained. These preliminary patterns appear to have still less differential beamwidth but more data are needed to completely evaluate this effect.

3.0 CROSSED WAVEGUIDE ELEMENTS

Crossed waveguide elements fed by coupling loops were selected as the radiating elements.* The outside depth of the waveguide as 0.8 inch with a 0.6 inch inside dimension. The loops were adjusted for good match and good cross-polarization isolation. Table 3-1 indicates the impedance match achieved. Figure 3-1 and 3-2 show the patterns of one element for each polarization with the element mounted in a 20-inch square ground plane. A complete set of these patterns was taken for all the elements and the patterns of the other elements are similar to the ones shown.

Table 3-1

Impedance Match of Loops in 0.8 Inch Long Crossed Waveguide Element

Loop	VSWR under 1.2	VSWR under 1.5
Upper	9360 to 9540 MHz	9210 to 9680 MHz
Lower	9350 to 9600 MHz	9270 to 9680 MHz

The E-plane patterns are quite broad, as expected for an open-ended waveguide in a reasonably large ground plane. Thus, if the elements can be properly impedance matched in the presence of mutual coupling from other elements, it should be possible to scan over a very large angle in this plane. The H-plane voltage patterns are approximately cos θ shaped, also as expected, and imply that wide angle scan will be more difficult in this plane.

*See Integrated Conformal Arrays, Quarterly Report, 2 March to 2 June 1970, Contract N00019-70-C-0397.

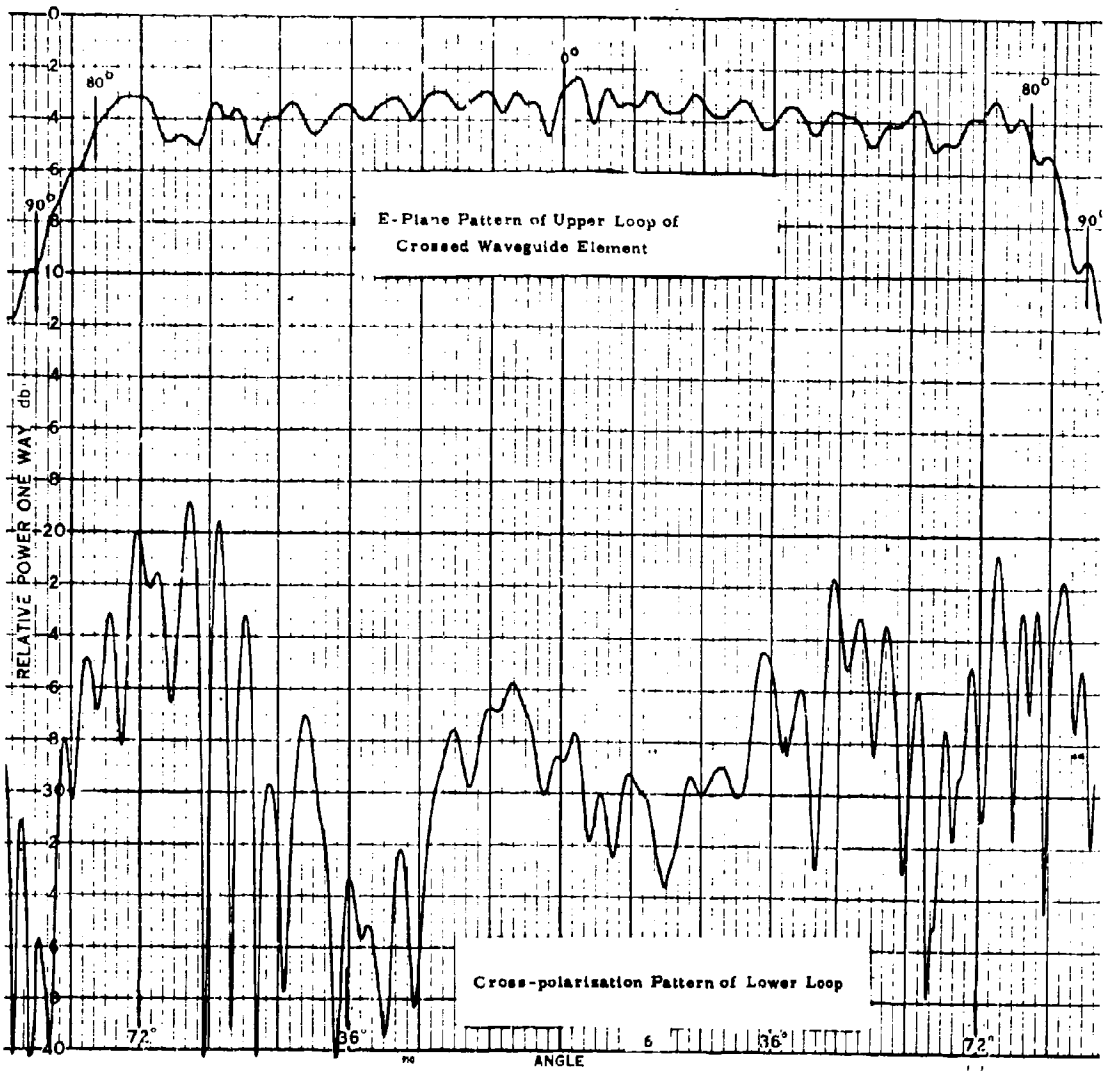
E-Plane Pattern of Upper Loop of
Crossed Waveguide Element
Cross-polarization Pattern of Lower Loop
RELATIVE POWER ONE WAY db
ANGLE
80°
90°
0°
72°
36°

Figure 3-1

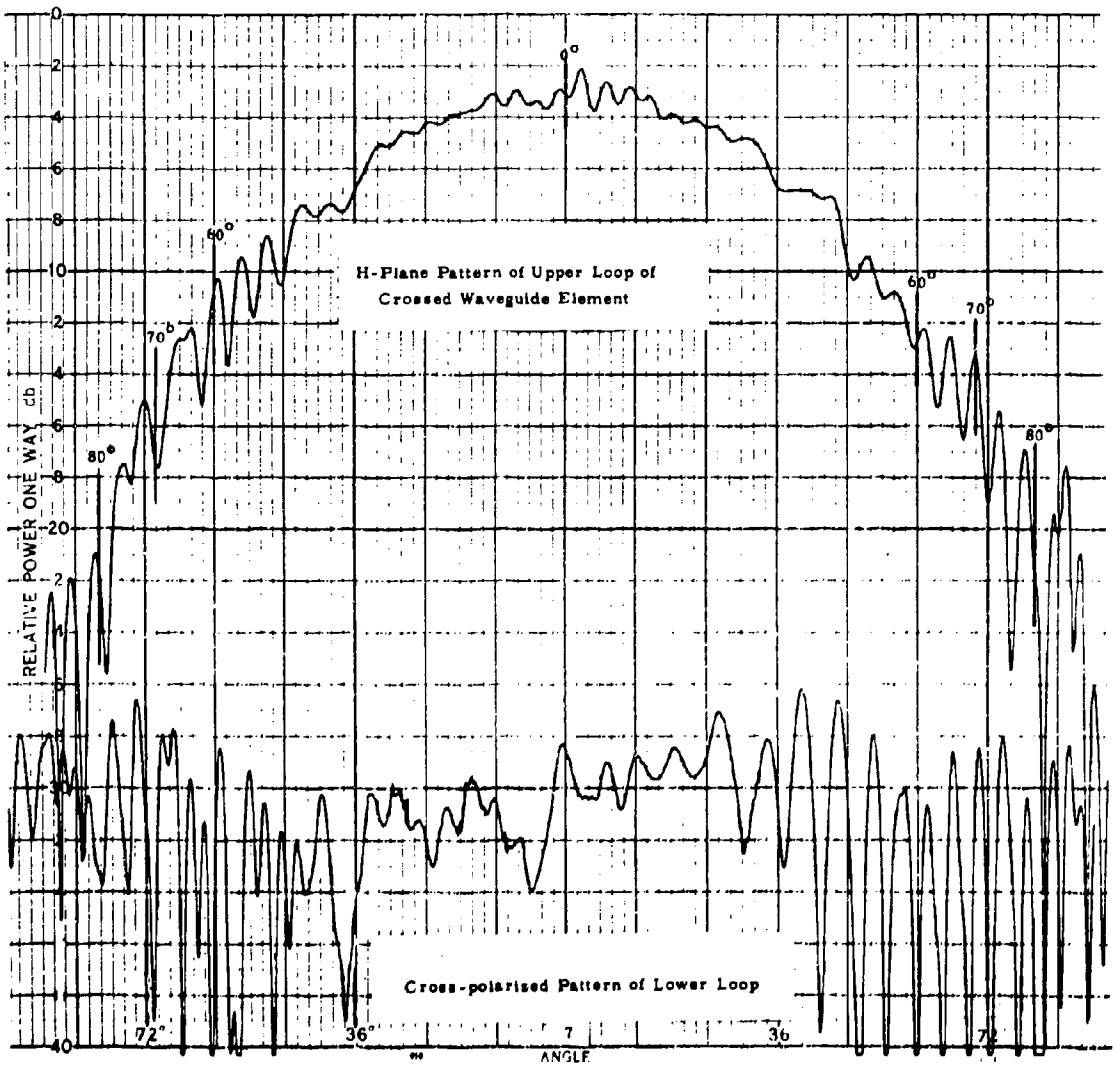
H-Plane Pattern of Upper Loop of
Crossed Waveguide Element
Cross-polarised Pattern of Lower Loop
RELATIVE POWER ONE WAY db
ANGLE
0°
60°
70°
80°
72°
36°

Figure 3-2

On each pattern a cross polarization pattern is given for the other terminal of the element. This gives a measure of the isolation between the two modes in the crossed waveguide and is on the order of 20 db over a wide scan angle for the E-plane pattern. Because of the cos θ shape of the H-plane voltage pattern, the isolation drops off with scan angle.

Although the inside depth of the element was only 0.6 inch, the tops of the squared-up loops were still almost 0.4 inch from the open end of the waveguide; therefore, it was decided to take off another 0.2 inch to see if such a short element could be matched. It turned out to be possible but difficult to get a match under these conditions. The loop had to be made with its short sides very near the walls of the waveguide. The proximity of this short section of the loop to the wall in essence produced a low impedance transmission line which it is believed acts as a matching transformer. As a result of the small spacing, the loop dimensions are quite critical. Therefore, if the crossed waveguide element is chosen as the type to be used on the conformal array, the extremely short element should be used only near the nose of the cone where space is at the greatest premium. An intermediate length of 0.5 inch for the inside depth probably would prove to be less critical in the loop adjustment and might be used for some or all of the rest of the elements.

4.0 ARRANGEMENT OF RADIATING ELEMENTS

In antennas that are electronically scanned the spacing of the elements becomes an important consideration. From the point of view of construction and electronic control some regular periodic structure is very desirable. In such a structure, however, if the spacing between elements is not sufficiently small, grating lobes will appear in the array pattern as it is scanned away from the broadside direction. Figure 4-1 shows the relative level of the endfire grating lobe vs. spacing for 8-element and 20-element uniform arrays for scan angles of 80° and 90°. Such grating lobes can be reduced by the use of non-periodic element spacing. However, because of the physical extent of the actual radiating elements, it may be difficult to achieve a significant amount of non-uniformity of spacing. This difficulty, together with the construction and control considerations mentioned above make it very attractive to attempt to find arrangements of elements that are geometrically regular and that will not give rise to grating lobes over the scan angles of interest. In the following section this problem is studied and several possibilities are considered for the crossed waveguide radiators.

4.1 GEOMETRICAL ARRANGEMENTS

The most compact arrangement of these elements on a planar surface is that shown in Figure 4-2. The elements are contiguous over most of their surfaces and are placed in an overlapping arrangement. In this arrangement the element centers lie on a square grid which is at an angle to the principal axes of the elements. The angle of tilt is a function of the wall thickness and the type of waveguide used for making the crossed waveguide element. The experimental elements built for the array discussed in Section 3.0 were all made from half-height X-band waveguide with a standard wall thickness of 0.050 inch. For these elements the grid is tilted at an angle of 24.8° and the distance between centers along the grid lines is 0.715 inch. In order to scan this array to endfire without the introduction of grating lobes, it would be necessary to keep the operating frequency at or below 7.43 GHz. This is well below the element design frequency.

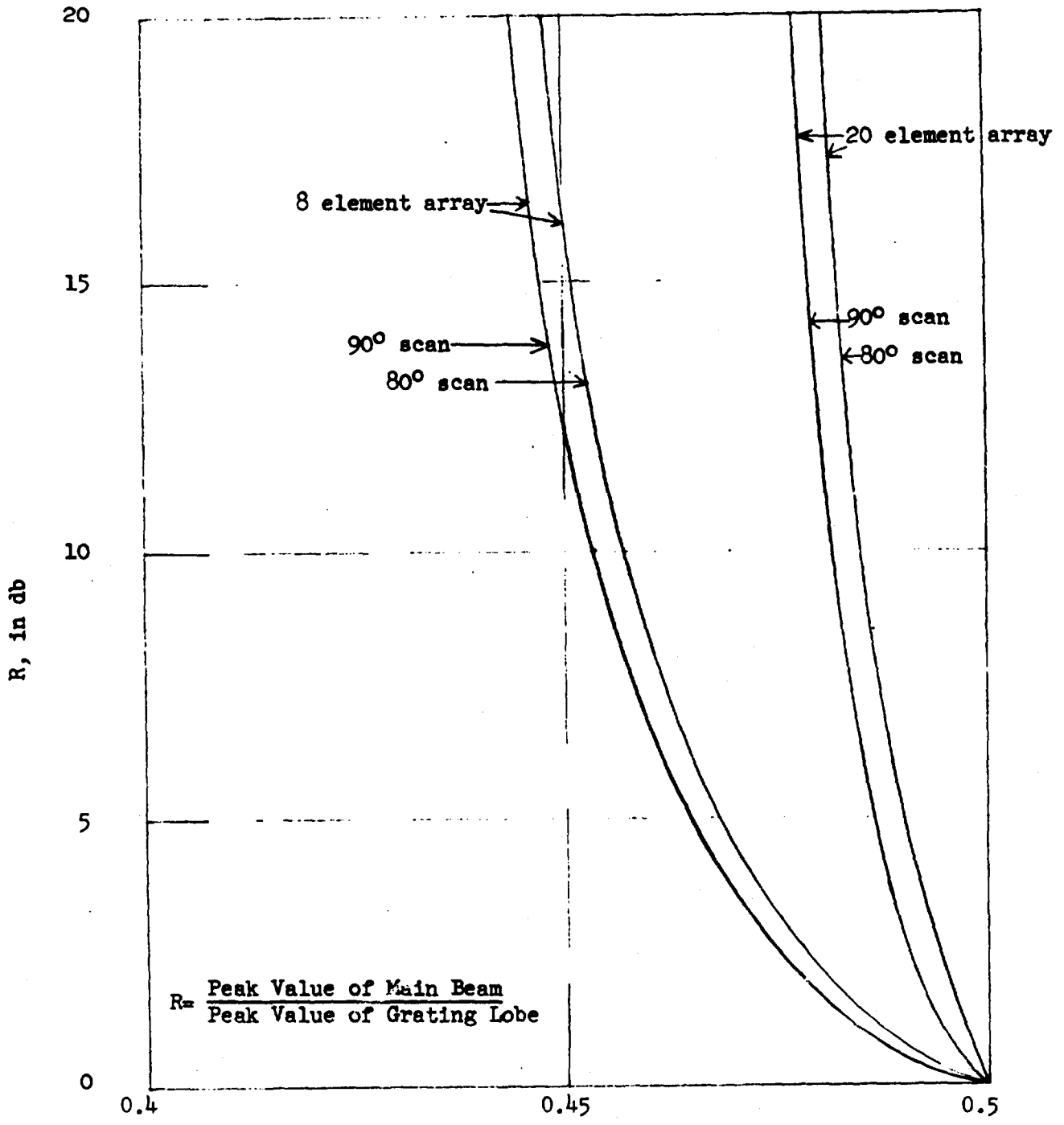

Figure 4-1. Grating Lobe Level vs. Interelement Spacing for Two Uniform Linear Arrays Scanned to the Vicinity of Endfire.

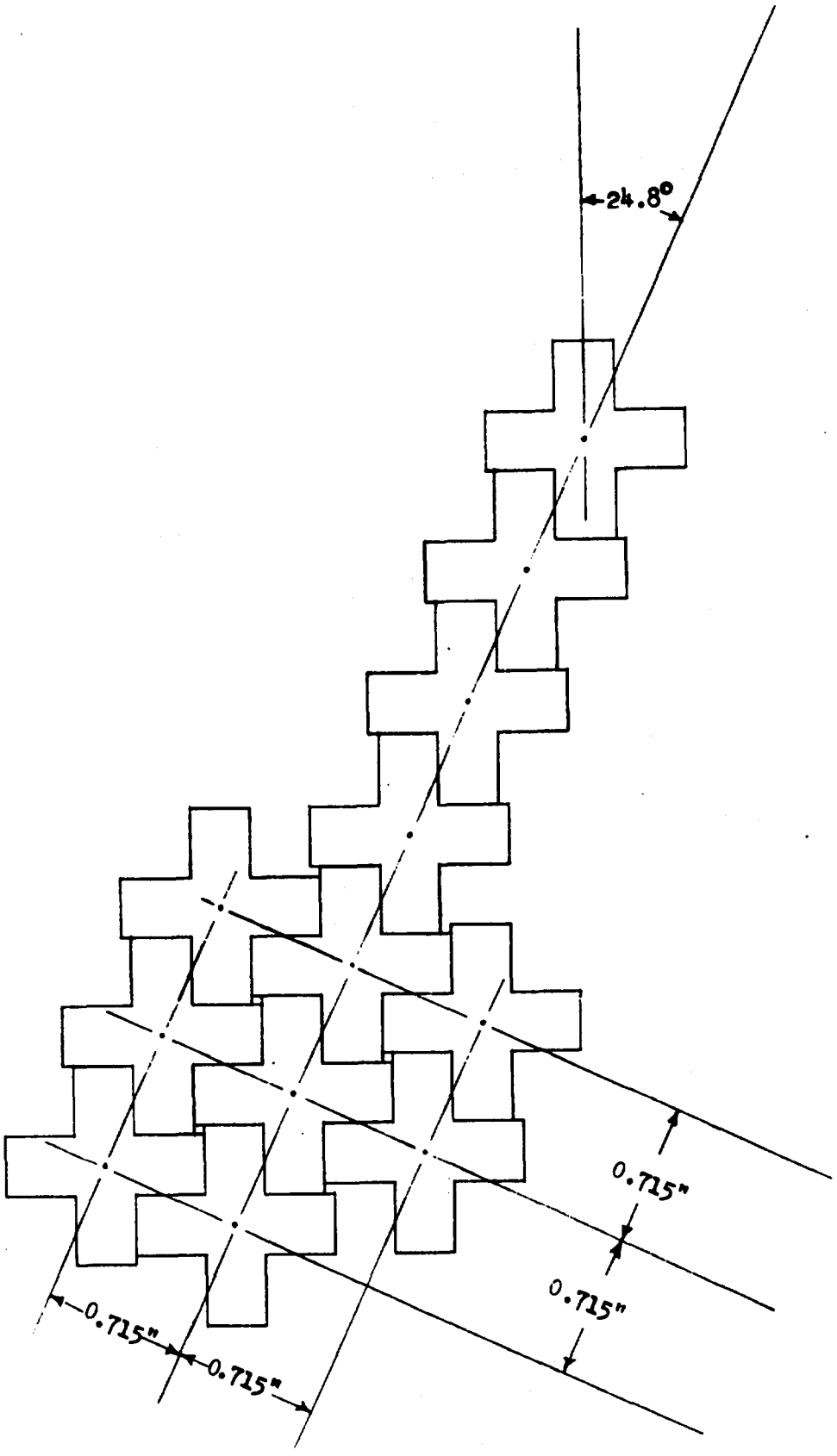

Figure 4-2. Illustration of Tilted Lattice for Closest Packing Arrangement of Crossed Waveguide Elements.

Although the arrangement shown in Figure 4-2 is the most compact arrangement possible for a two dimensional array, it has certain drawbacks that make desirable a study of other arrangements. First, the axes of the most readily identifiable linear arrays do not coincide with either the E-plane or the H-plane of the radiation from the arms of the radiating element. This property will lead to control complications when such an array is placed on a cone because it will be most natural to arrange the linear arrays along the cone generatrices with excitation specified in terms of radial and circumferential components.

It is a relatively simple matter to arrange the elements in a staggered manner with relatively small spacings in the plane containing the scan axis. Several such possible arrangements are shown in Figures 4-3 and 4-5. In these arrangements the elements are oriented so that their E- or H-planes lie in the scan plane and hence avoid the problems mentioned above. However, as can be seen in the Figures, each arrangement presents some lattice dimension that is greater than the 0.715 inch square lattice of Figure 4-2. In Figure 4-4 it is evident that in the diagonal planes the array appears as an array of element pairs. The two elements in a pair are separated by 0.119 inch and the pairs are separated by a spacing of 0.793 inch. Thus, though in the principal planes the spacing is less than in Figure 4-2, the diagonal spacing is greater. The element pairs provide some grating lobe suppression but not sufficient to offset the increased spacing. The grating lobe suppression for this array is shown in Figure 4-6. The arrangement shown in Figure 4-5 has similar problems. In spite of the increased diagonal spacing of such arrays, however, a staggered "linear" array similar to a portion of Figure 4-4 was selected to be assembled for experiments to illustrate beam scanning toward end-fire and to determine mutual coupling effects (see Figure 4-7). This arrangement permits operation at 8.16 GHz which is just below the lower end of X-band and well within the operating capability of X-band components.

The difficulty with achieving sufficiently small spacing to preclude grating lobes at the desired operating frequency in X-band could be resolved by shrinking the element dimensions. This approach may require the use of dielectric-loading to achieve proper element spacing. The use of random

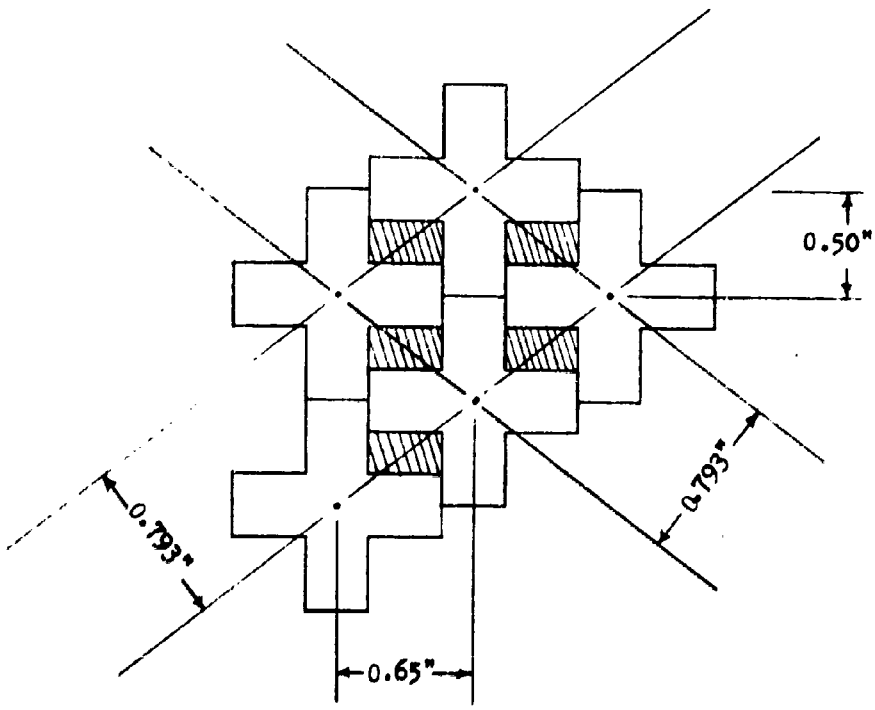

Figure 4-3. A Method of Staggering the Elements in a Non-Optimum Packing Arrangement

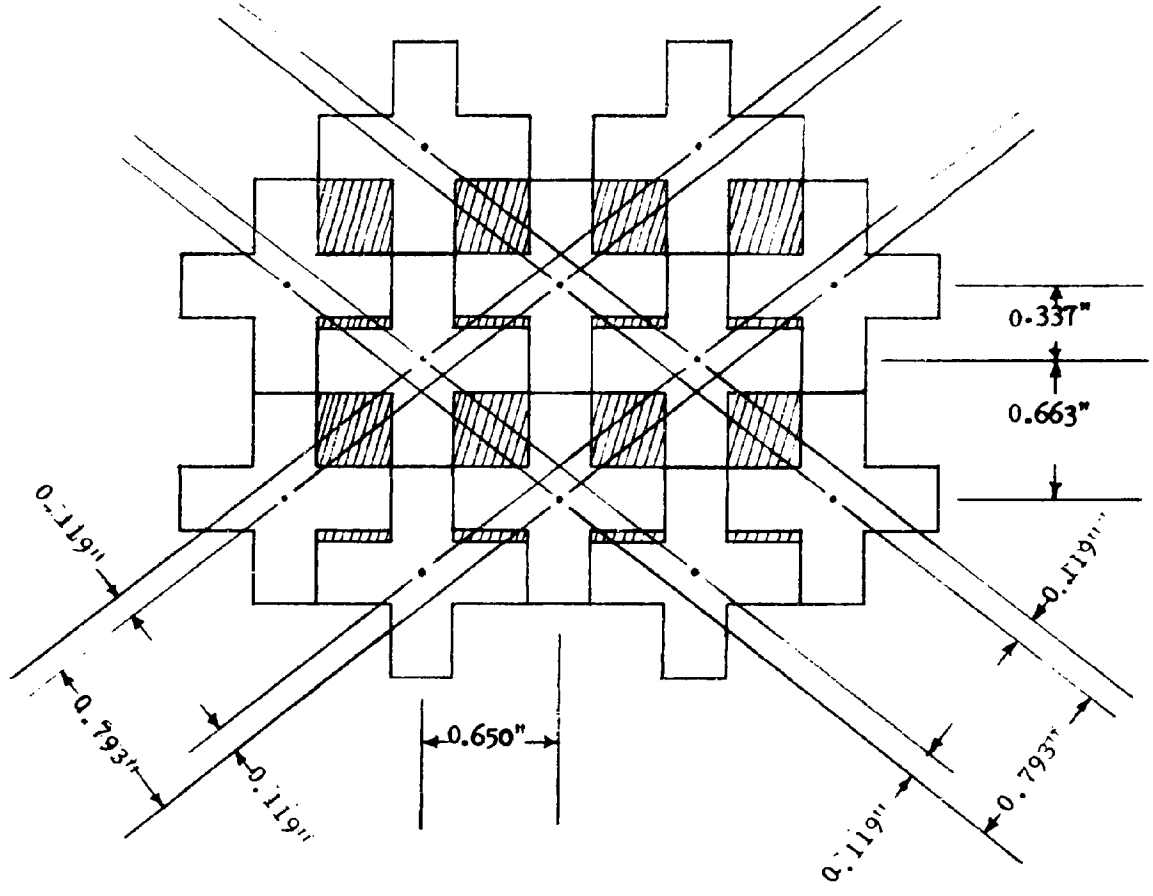

Figure 4-4. A Non-Symmetrical Staggered Arrangement

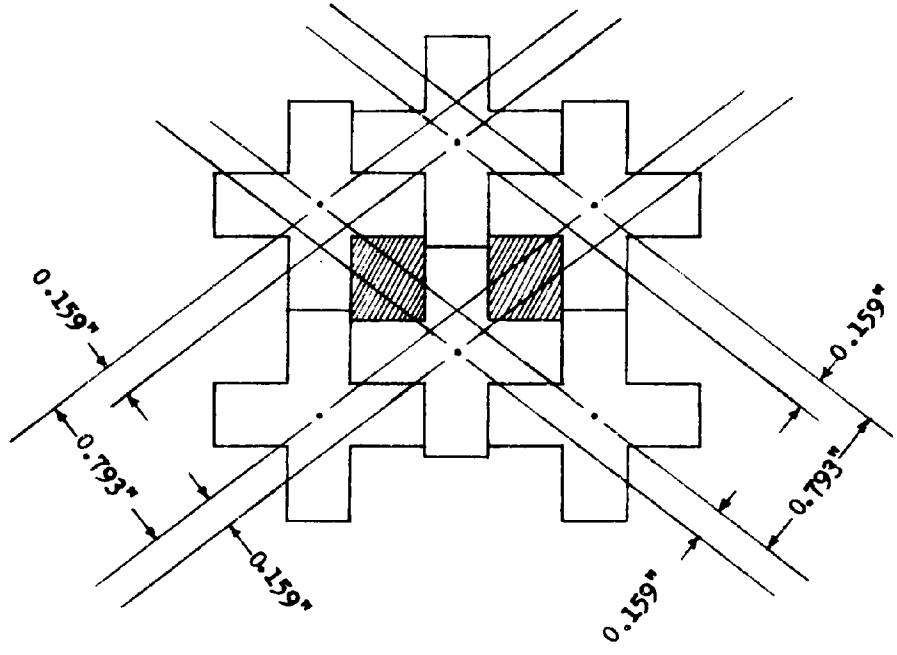

Figure 4-5. A Slightly Different Version of the Configuration Shown in Figure 4-4.

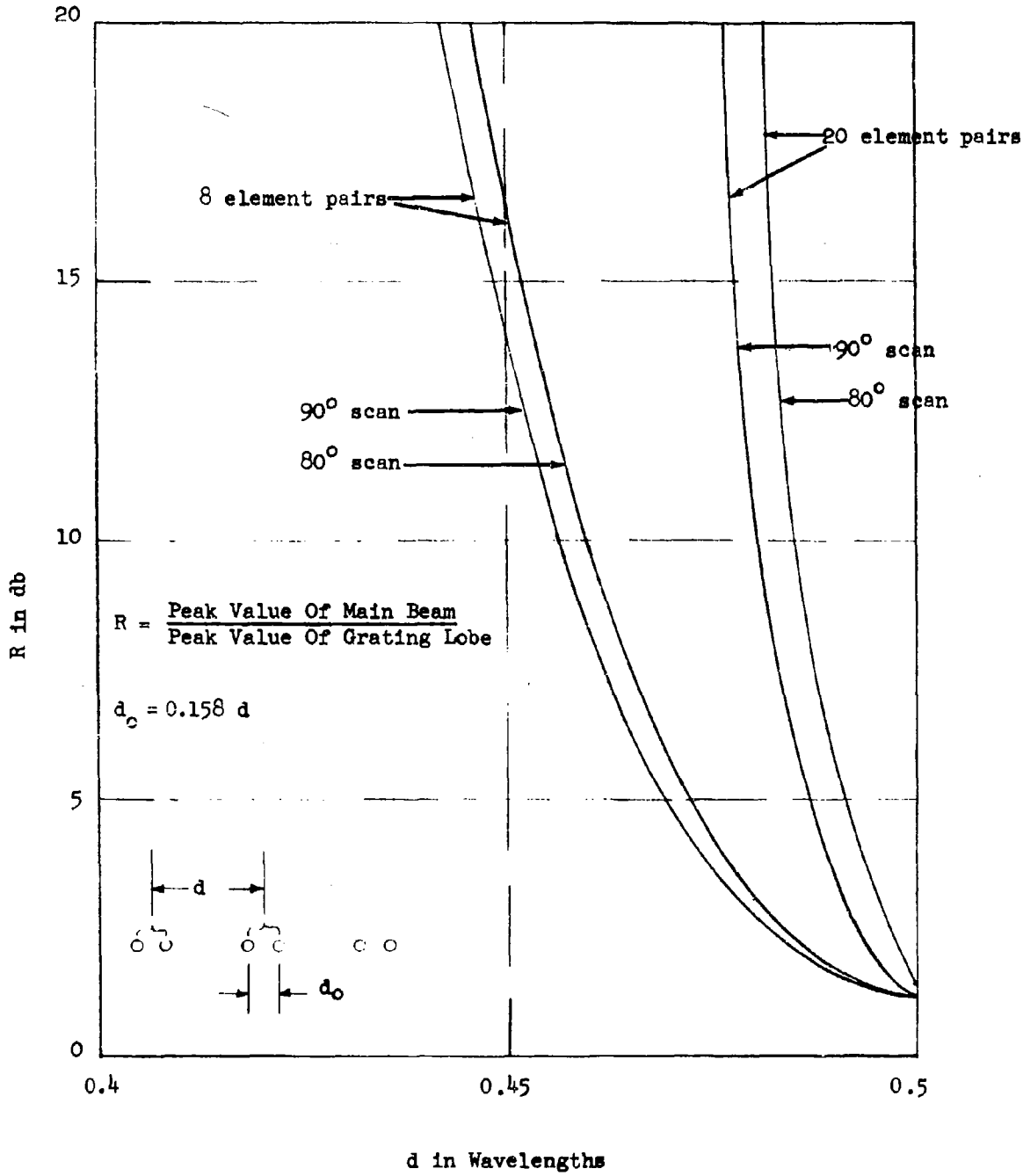

Figure 4-6. Grating Lobe Level vs. Spacing Between Pairs of Elements for Two Linear Arrays Scanned to the Vicinity of Endfire

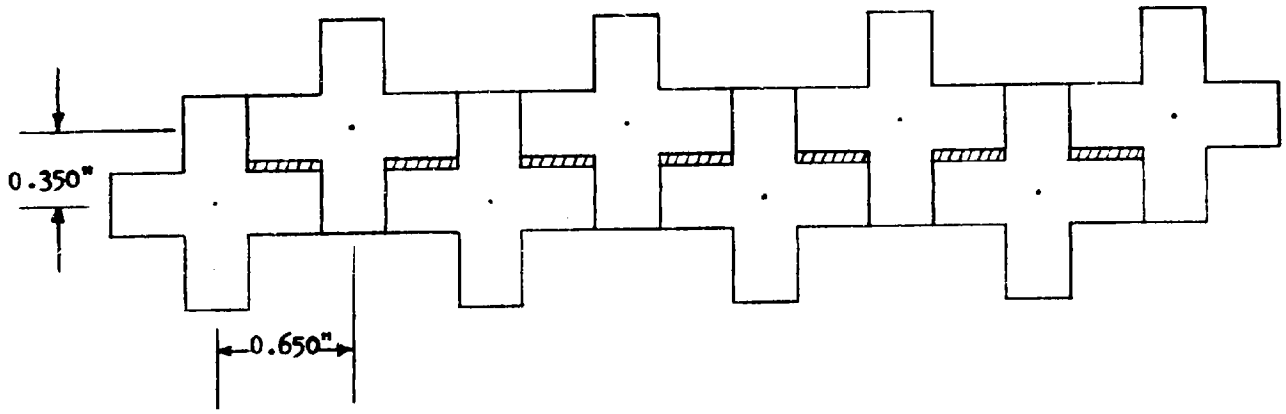

Figure 4-7. Selected Configuration for Scanned Linear Test Array

spacing between elements is another possible method of reducing grating lobes. However, in view of the limited space on the cone, the ability to place the elements in a truly random fashion is limited. A third possible method of reducing grating lobes lies in making use of the circular symmetry of the cone and arranging the elements in a particular staggered configuration. This plan is discussed in detail below.

4.2 APPROXIMATE ONE-DIMENSIONAL SCANNING

In the conical array one can take advantage of the circular symmetry of the surface to reduce the steering problem essentially to that of scanning in one dimension only. Figure 4-8 shows an end-on view of the cone with the shaded portion representing the excited area of the surface. If the beam lies in the plane perpendicular to the cone axis, its position will be as shown in the figure — and symmetrical with respect to the active area of the array. If the beam is scanned toward endfire while ϕ_1 is held fixed, it can be seen that the projection of the beam onto the plane of the paper will still fall at ϕ_1. Hence, the active area is still symmetrically located with respect to the beam. The beam can be thought of as being broadside to the cone in the ϕ plane and capable of being electronically scanned in the plane that passes through the cone axis (the θ plane).

If the beam is now steered around in the ϕ plane to ϕ_2, ideally the active portion of the array will follow it to maintain a symmetrical relationship with the new beam pointing direction as shown in Figure 4-9. Here also, the beam can be electronically steered toward endfire without changing the angle ϕ_2 or disturbing the symmetry conditions. Hence, we can conclude that for any angle of ϕ, in the ideal case of a continuously illuminated aperture, the beam can be considered to be broadside to the cone in the ϕ plane and need be electronically scanned only in the θ plane.

With a discrete number of elements on the cone we can only approximate the ideal situation outlined above. However, if a reasonably large number of elements are used, the approximation will be quite close. For example, if 16 elements are used in the larger rings around the cone, the largest portion of the area of excitation can be switched in $22\frac{1}{2}$-degree

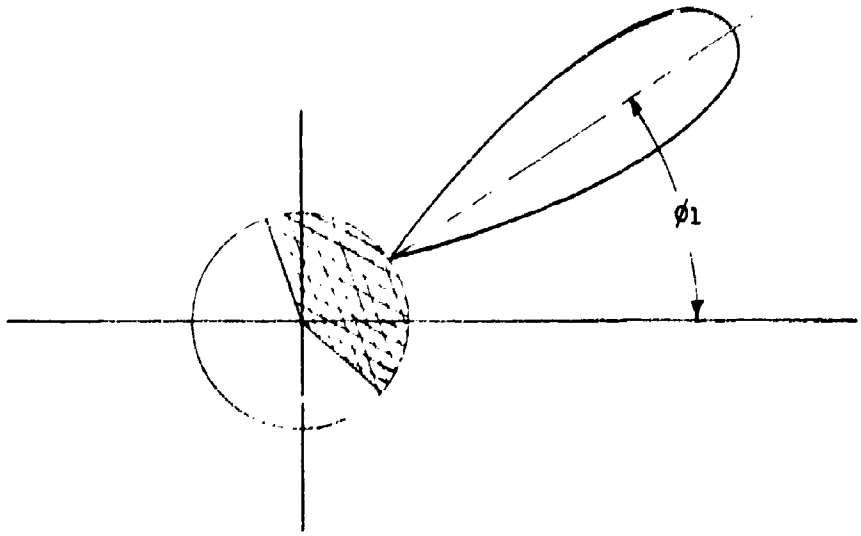

Figure 4-8. Excited Portion of Cone for Beam Pointing to ϕ_1.

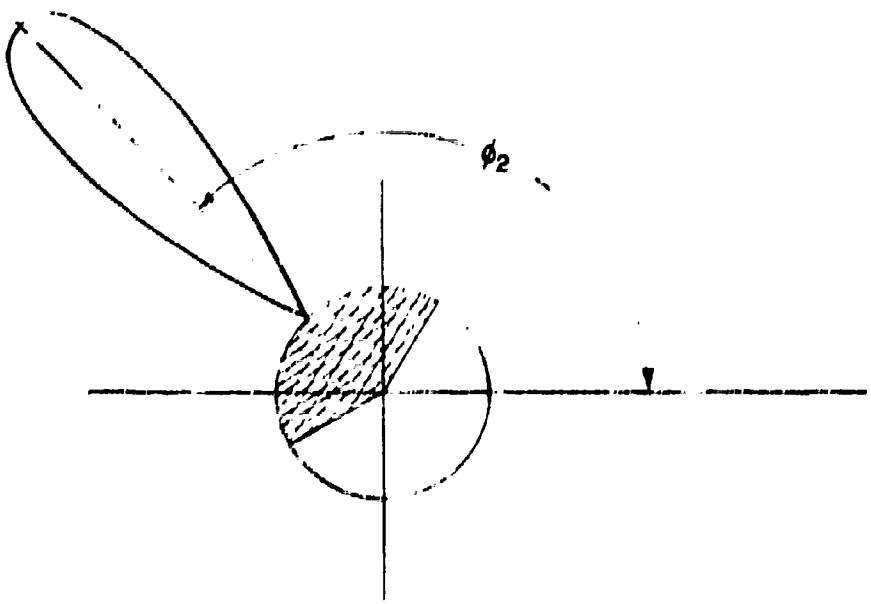

Figure 4-9. Excited Portion of Cone for Beam Pointing to ϕ_2.

steps. Thus, it is necessary to electronically scan the beam only $\pm 11\frac{1}{4}$-degrees off the perpendicular to the excited area to achieve full coverage around the axis of the cone by a sequence of switching and phasing operations. This concept has been applied to a cylindrical array at the Hughes Aircraft Company on another program and the array is called a switched-beam phased array. Since any one active area of the cone scans only $\pm 11\frac{1}{4}$-degrees in the ϕ plane, the interelement spacing in that plane need be only slightly less than the spacing required for an array that does not scan at all in that plane. Hence, the interelement spacing problem is reduced approximately to that associated with scanning in the θ plane only.

Cylindrical arrays that are phased to produce narrow beams tend to be more susceptable to grating lobe problems than do comparable planar arrays. This results from two factors: (1) on the sides of the active portion of the array the element patterns do not point in the direction of the beam; and (2) in this same region it is necessary to introduce a large interelement phase shift into the excitation to compensate for the curvature of the cylinder. The latter factor is equivalent to scanning the side portion of the array to some angle off the normal to the cylinder at that point; hence, the interelement spacing must be kept correspondingly small to prevent the formation of grating lobes.

The conical array can be thought of as a set of cylindrical arrays of different radii as a first order approximation. Hence, it is to be expected that it, too, will have a tendency to have grating lobes in the ϕ plane. Therefore, it is anticipated that the interelement spacing in that plane will have to be kept smaller than would normally be necessary for an equivalent planar array. However, the fact that each circle of elements on the cone nearer the tip is smaller than the previous one may tend to alleviate this problem by introducing a modest amount of non-uniformity into the element placement.

A more nearly continuous illumination in both principal axes of the cone can be achieved by staggering the elements in alternate circles as shown in Figure 4-10. Thus, although the actual spacing between any two elements on an 8" diameter circle is $1.2\lambda_o$ (assuming 16 elements

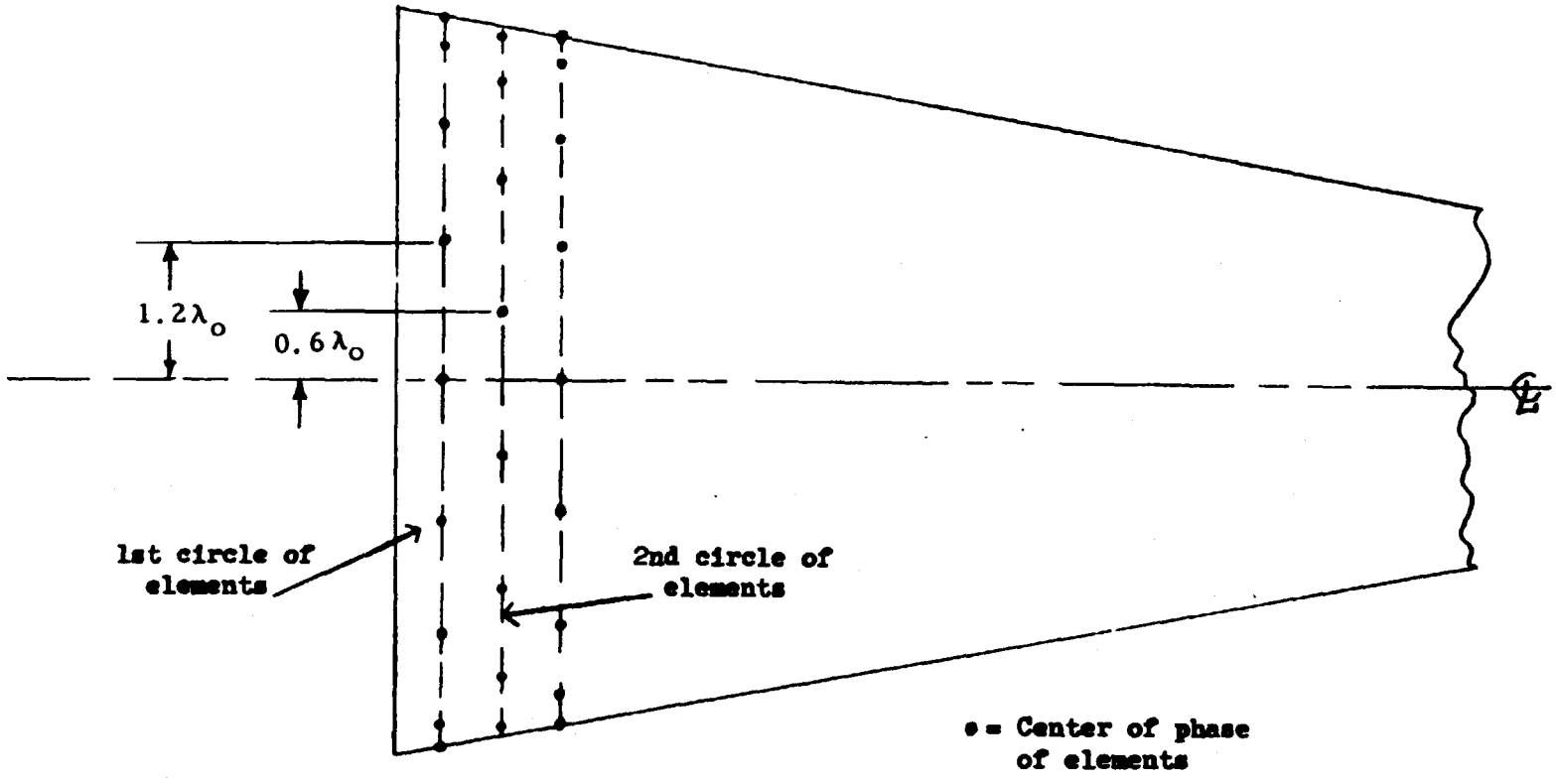

Figure 4-10. Effect of Staggering the Elements in Alternate Circles on the Cone

per circle) the effective spacing is only one-half that value. An interelement spacing of 0.6 λ_o is rather large for a circular array; however, each circle nearer the tip of the cone will bring the elements closer together until we get to the point of physical interference. Hence, the average interelement spacing in the ϕ plane for the section of the cone that has 16 elements per ring should be less than 0.5 λ_o.

In the smaller regions of the cone fewer elements will be needed per circle. The type of element to be used will influence the decision on just how many should be used in each circle. The crossed waveguide elements developed in this program can be fitted together quite closely on a flat surface provided they are rotated at an angle of approximately 20-25 degrees, depending on wall thickness, to the principal axes of the lattice (see Figure 4-2). They can brought most closely together on a curve surface if they still maintain that angle. When the elements in alternate circles are staggered in a symmetrical fashion, the lattice is rotated 45^o as shown in Figure 4-11. When large interelement spacing is used (as on the larger circles), the arrangement shown in Figure 4-12 results. This figure represents the largest circle of elements on an 8-inch cone. Here the interelement spacing is sufficiently great that any angular orientation of the elements could be used. Since they must be angled at $20\text{-}25^o$ for the smaller circles, though, the same rotation is carried through to the larger circles.

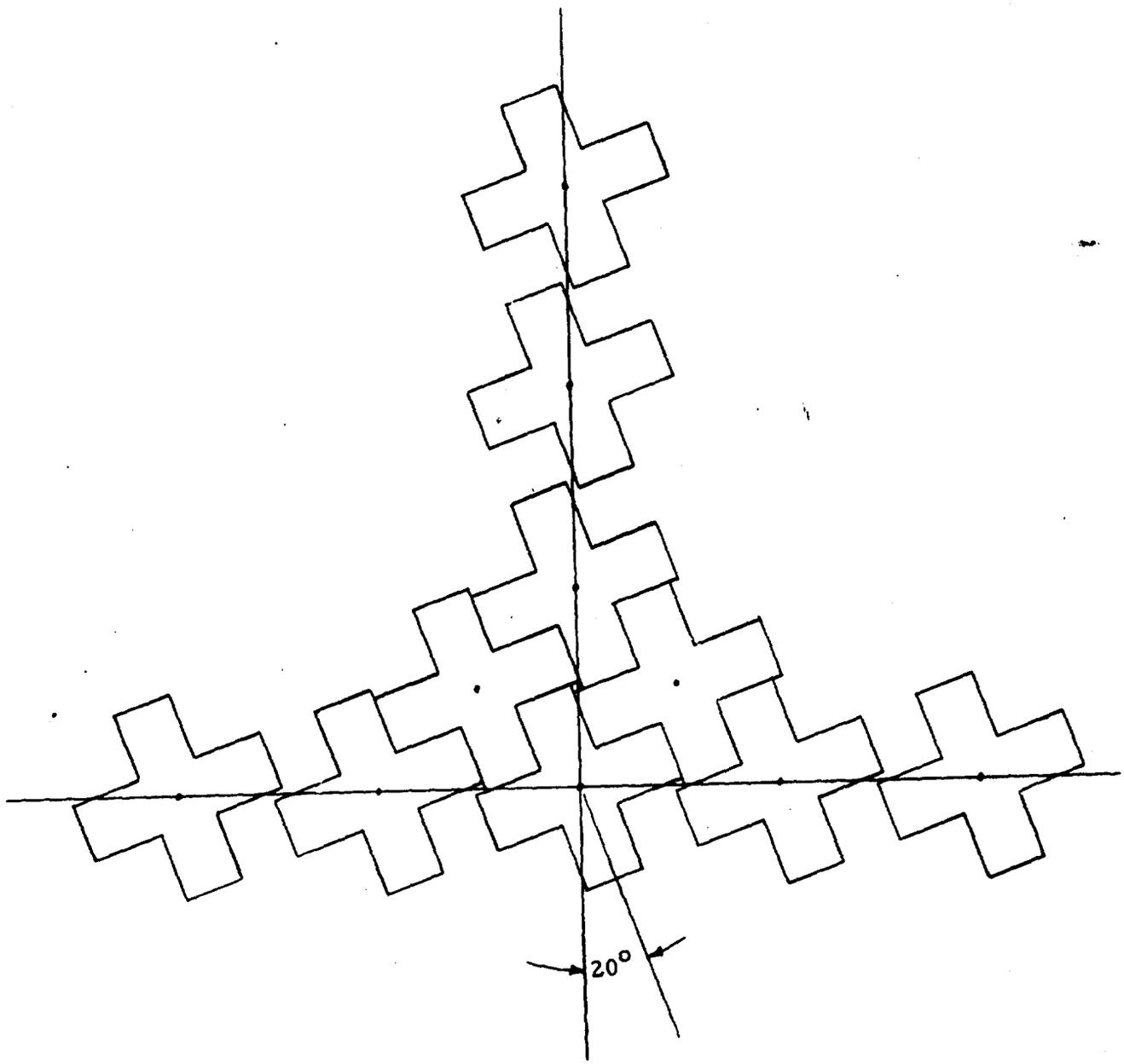

Figure 4-11. Closest Packing of Crossed Waveguide Elements Occurs When They Are Tilted at an Angle of Approximately 20° in Staggered Arrangement.

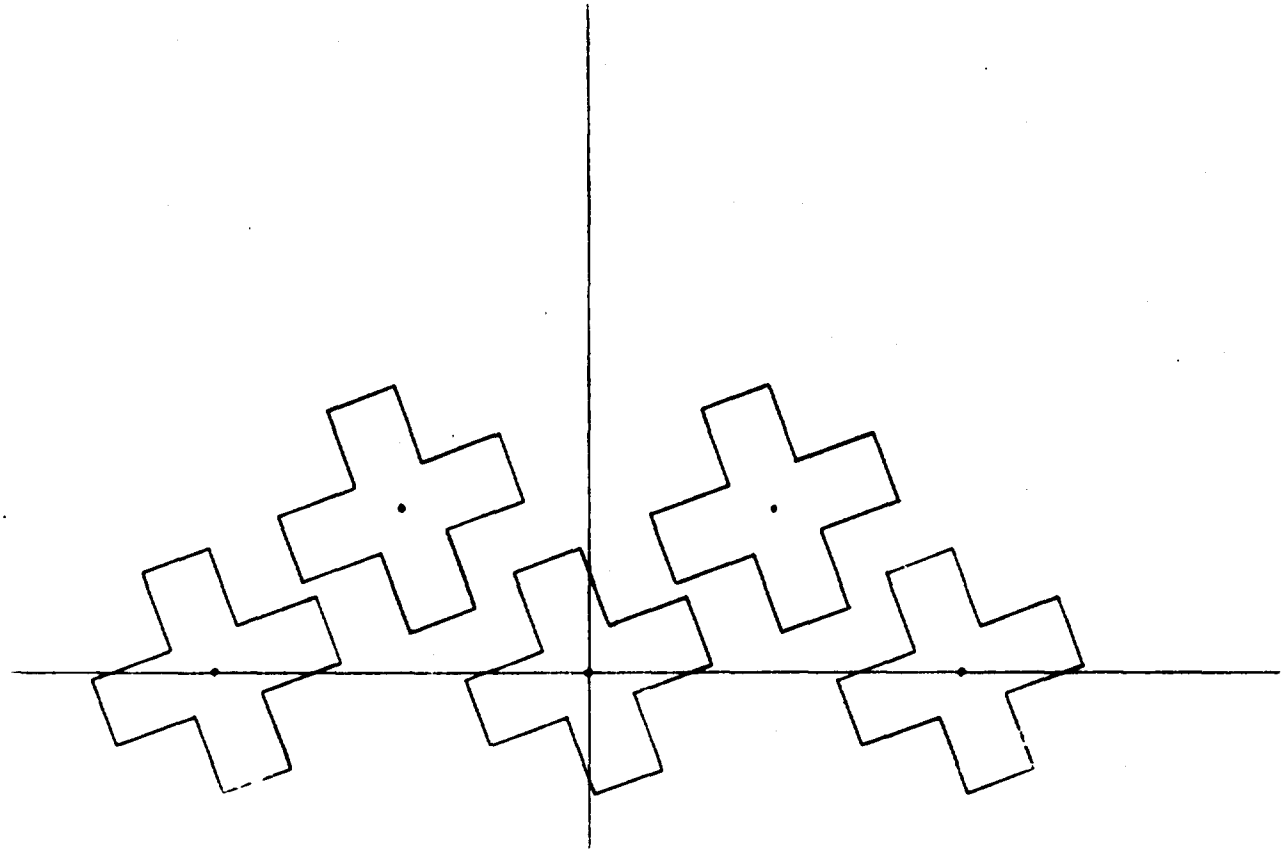

Figure 4-12. Typical Spacing Between Elements of the First Two Rows of Staggered Arrangement at Large End of Cone

5.0 EXPERIMENTAL ARRAY

The crossed waveguide elements were arrayed on a ground plane to obtain a feeling as to their performance in a phase scanned linear array. Eight radiating elements were arrayed as shown in Figure 5-1. The elements were matched individually and then fitted into the ground plane. The gaps between slots visible in the photograph were filled with conducting tape. One half of each element was terminated in a matched load. The other half, that part of the cross perpendicular to the axis of the array, was connected to an r-f chain consisting of a coax-to-waveguide transducer, a slide-screw tuner, a slotted line, a precision attenuator and a precision phase shifter. A corporate feed consisting of waveguide bends, sections and magic tees was connected to each phase shifter. The various components are visible in Figure 5-2. The radiating elements were essentially fed by independent coherent generators due to the inherent isolation in the corporate feed; thus there was no coupling between radiators through the feeding network.

The ground plane was in the shape of a flat plane with cylindrically shaped wings. These wings and the small pieces of absorber, as shown in Figure 5-3, were used to reduce the reflections from the edges of the ground plane.

The linear array could be phased to direct a beam in any arbitrary direction and each radiating element could be matched individually. An arbitrary amplitude taper could also be programmed.

For the particular experiments to be discussed uniform illumination was employed. The array was used in the transmitting mode to facilitate the matching and impedance measurements. The polarization was parallel to the axis of the array; the frequency used was 8.18 GHz.

Two different conditions were programmed into the array. In the first one, all radiating elements were matched in the presence of the others for the main beam of the array pointing at broadside. Then the array was scanned toward end-fire in 10° steps. In the second condition, the radiating elements were matched at 80° (10° from end-fire) and the array was then scanned toward broadside. The matching for each initial

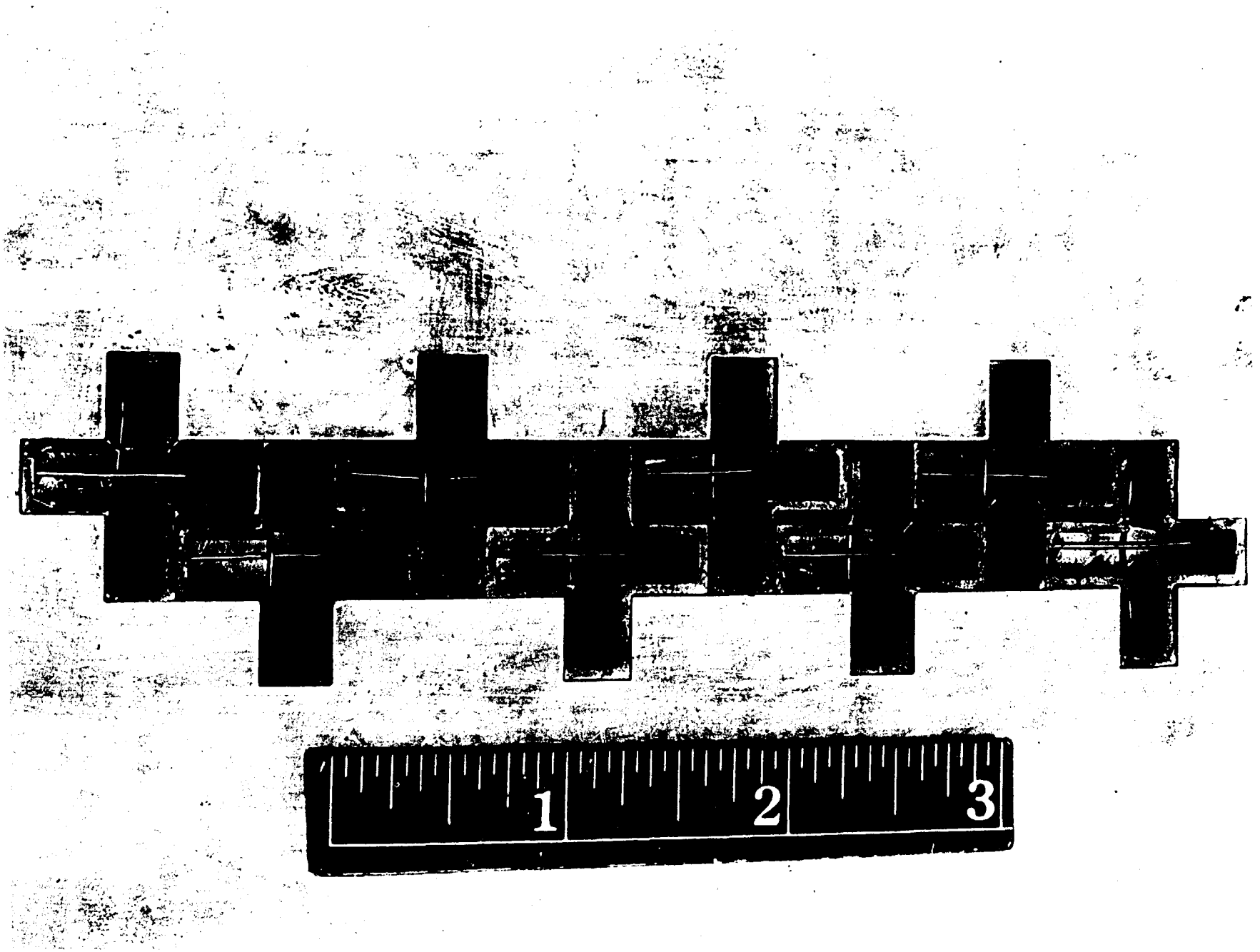

Figure 5.1 Eight-Element Linear Array Using Crossed-Slots

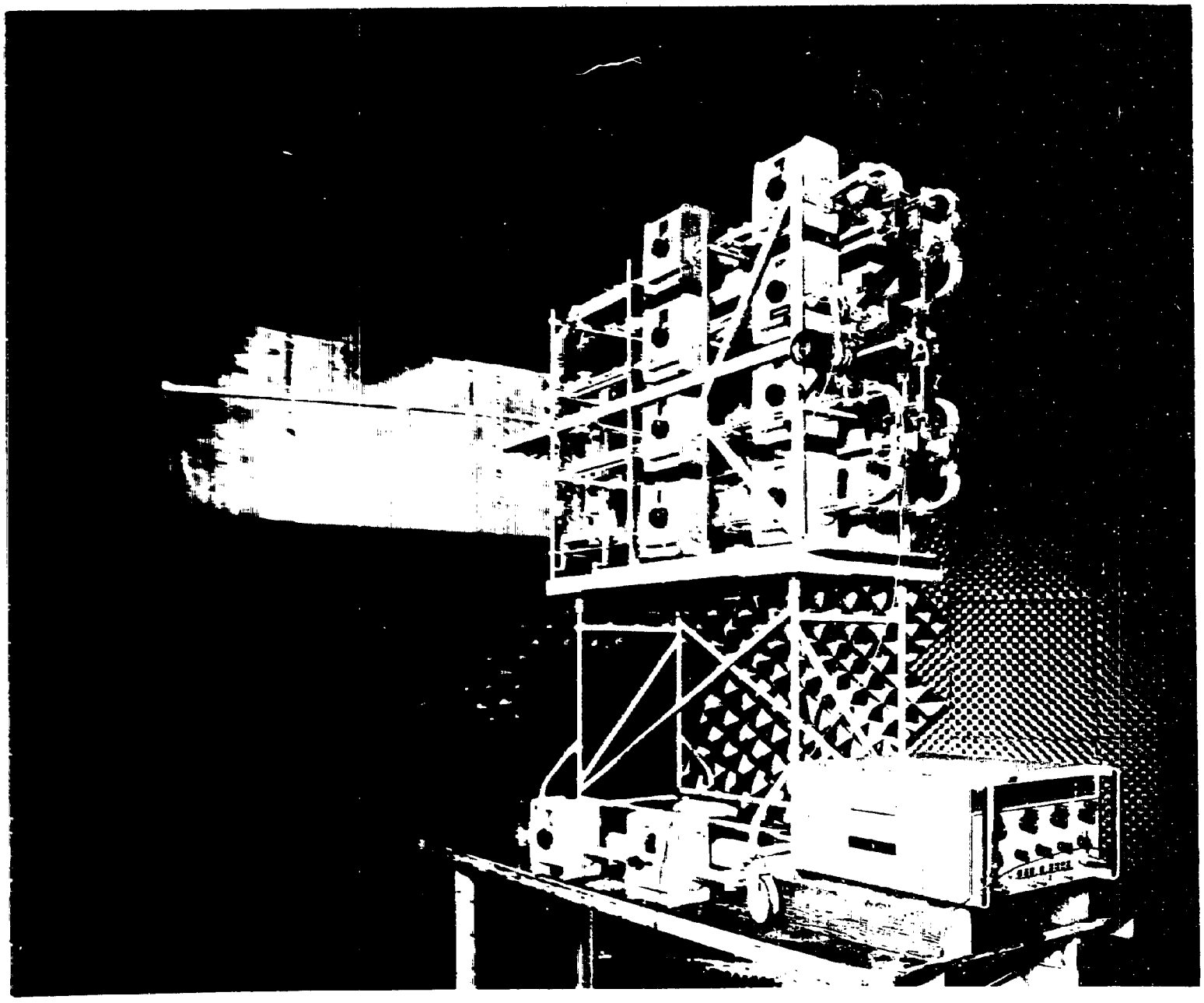

Figure 5-2. Array Mounted in Ground Plane - Back View

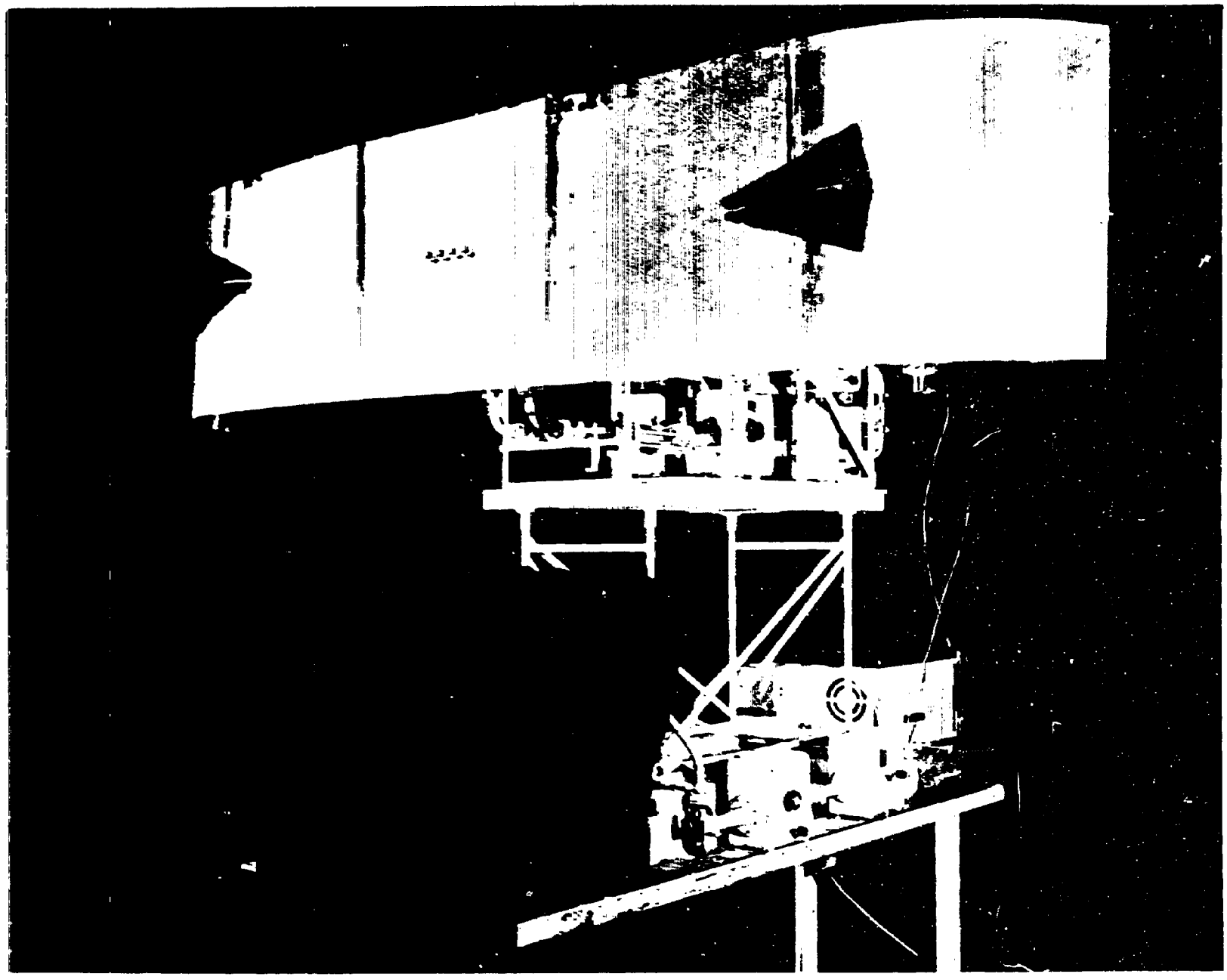

Figure 3-3. Array Mounted in Ground Plane - Front View

condition required an iterative procedure because of the mutual coupling between elements; three iterations were sufficient in each case. The elements were then phased to produce a pencil beam in the required direction (0^{o} to 80^{o}). The phase shift required at every element for each 10^{o} step in the scan of the pencil beam was calculated theoretically and then added to the initial setting of the phase shifter. No other adjustments were made. Individual element patterns were also taken.

5.1 ARRAY PATTERNS

The scanned patterns for the array are shown in Figure 5-4 through 5-13. Two sets of patterns are shown. The first set shows the array matched at broadside and scanned to 90^{o} (Figure 5-4 through 5-8). For the second set the array is matched at 80^{o} and scanned to broadside (Figure 5-9 through 5-13). In each figure the theoretical calculated pointing direction is indicated by a line and labeled by the appropriate angle. The patterns follow the theoretical predictions quite well from broadside to 80^{o} (10^{o} from the surface of the ground plane). The pattern did not scan beyond 80^{o}. The sidelobe levels were satisfactory through the scan range. The shapes of the sidelobes appeared better behaved when the array was matched at broadside. The peak of the main beam decreased by about 3.6 dB as the beam was scanned from broadside to 80^{o} when the array was matched at broadside. For the array matched at 80^{o} the change in the peak of the main beam was about 1.6 dB. The VSWR's under matched conditions ranged from 1.01 to 1.05. The VSWR's measured from 80^{o} from the matched condition ranged from 1.6 to a maximum of 4.5 depending on the element.

As expected the element patterns were symmetrical for the center elements and asymmetrical for the end elements. The individual patterns are shown in Figures 5-14 and 5-15. The patterns of the symmetrically placed slots are images of each other. The patterns were quite similar for the two matched cases.

Thus, it is concluded that this array can be scanned to 10^{o} from end-fire for the polarization chosen.

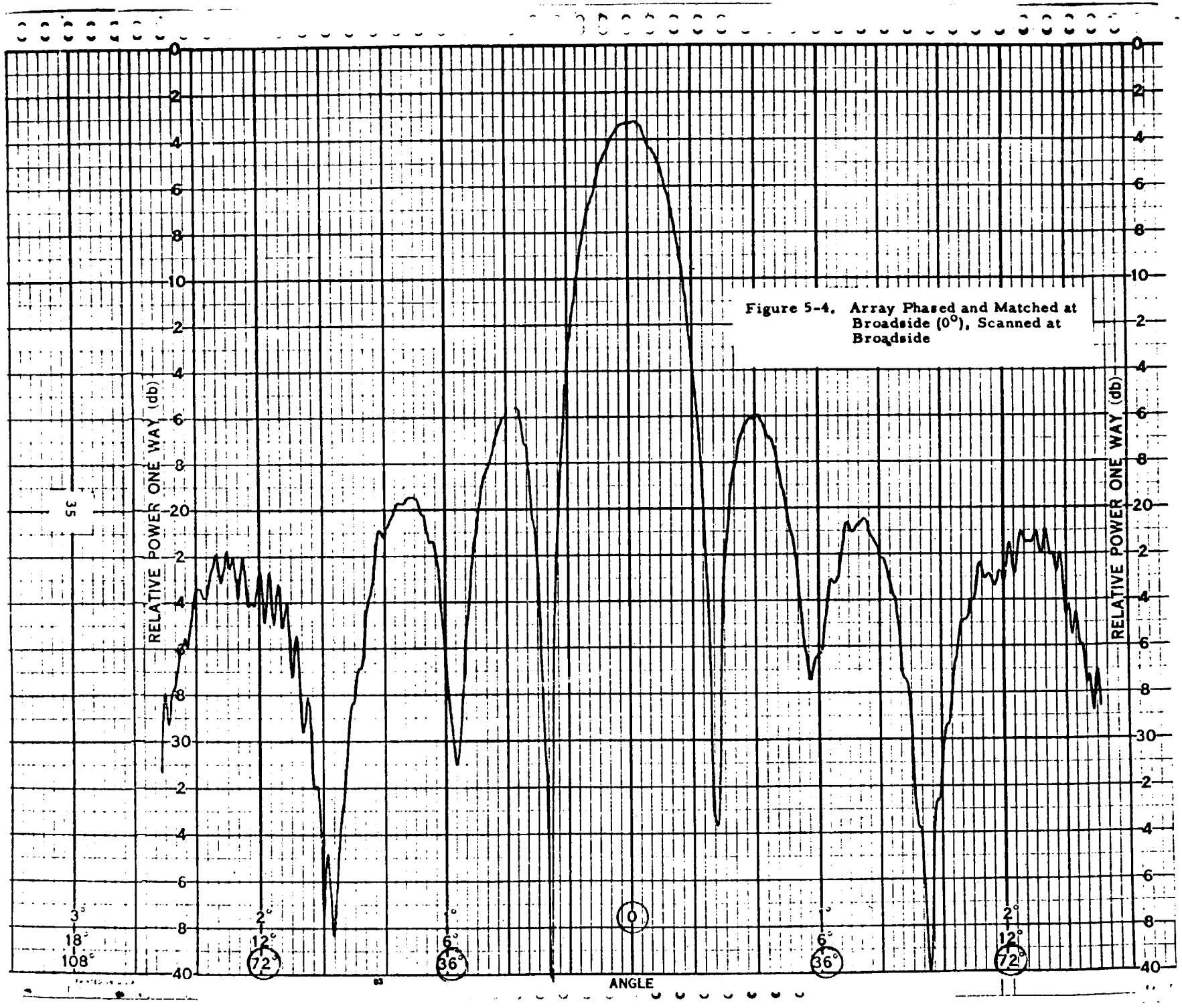

Figure 5-4. Array Phased and Matched at Broadside (0°), Scanned at Broadside

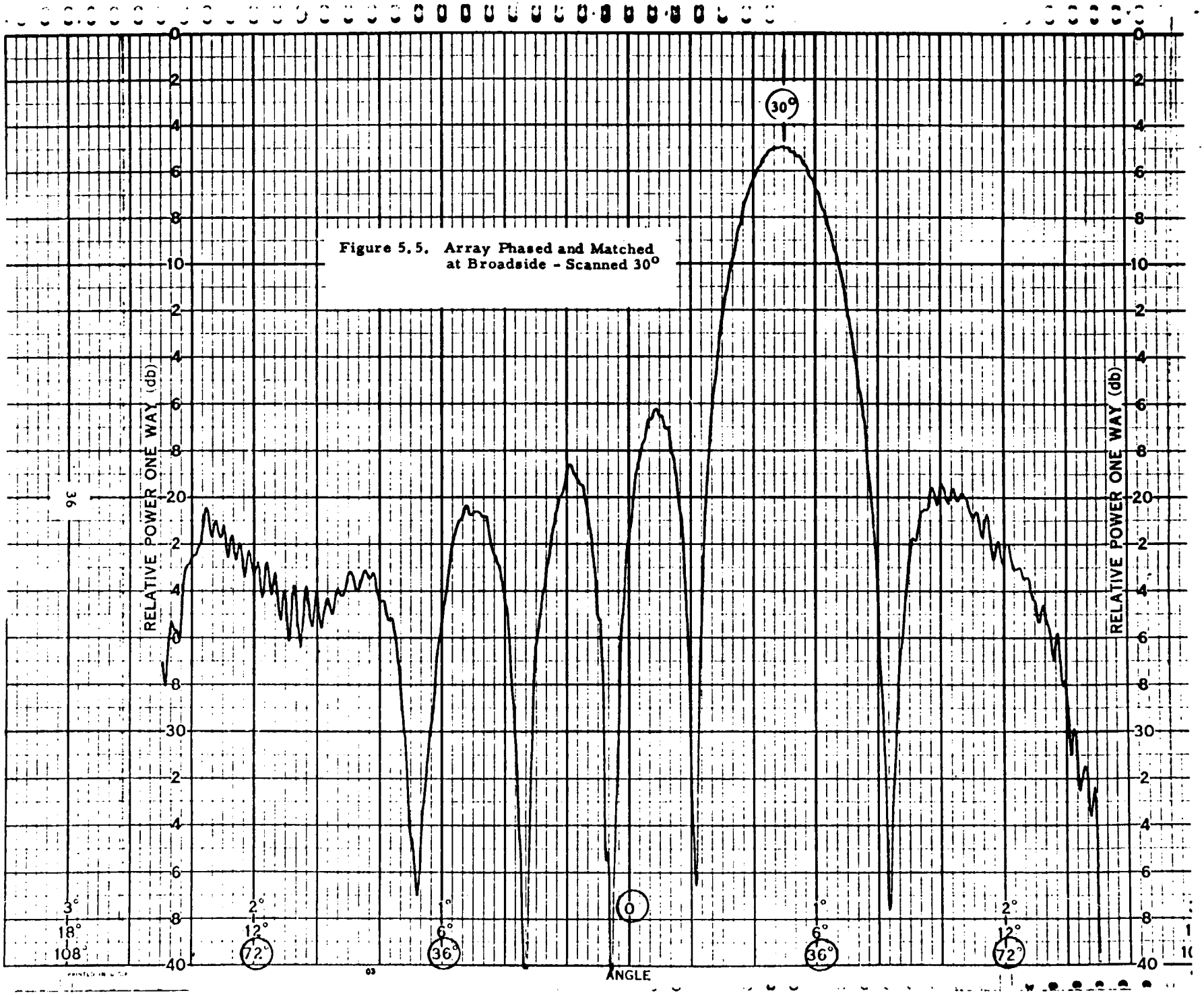

Figure 5.5. Array Phased and Matched at Broadside - Scanned 30°

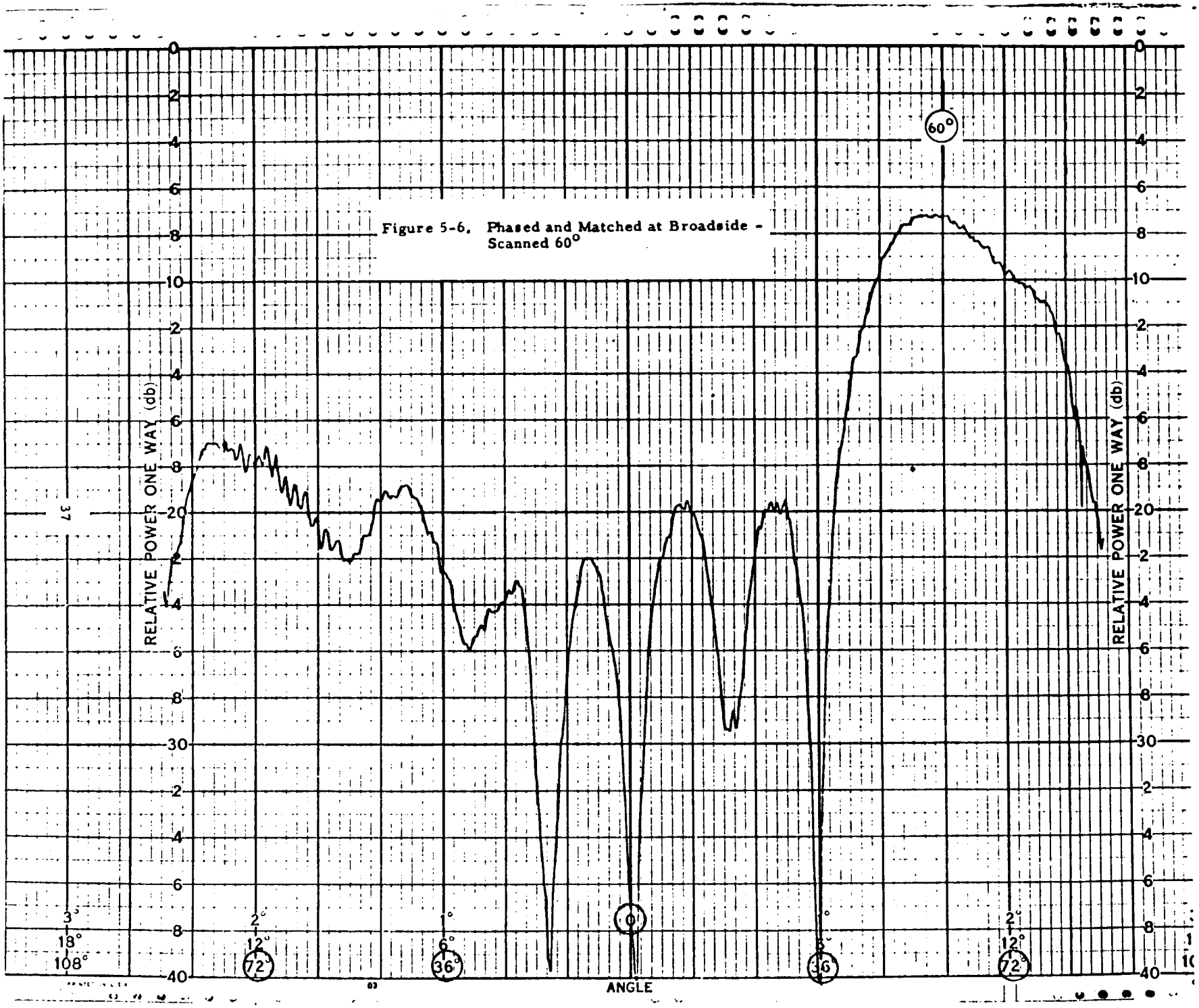

Figure 5-6. Phased and Matched at Broadside - Scanned 60°

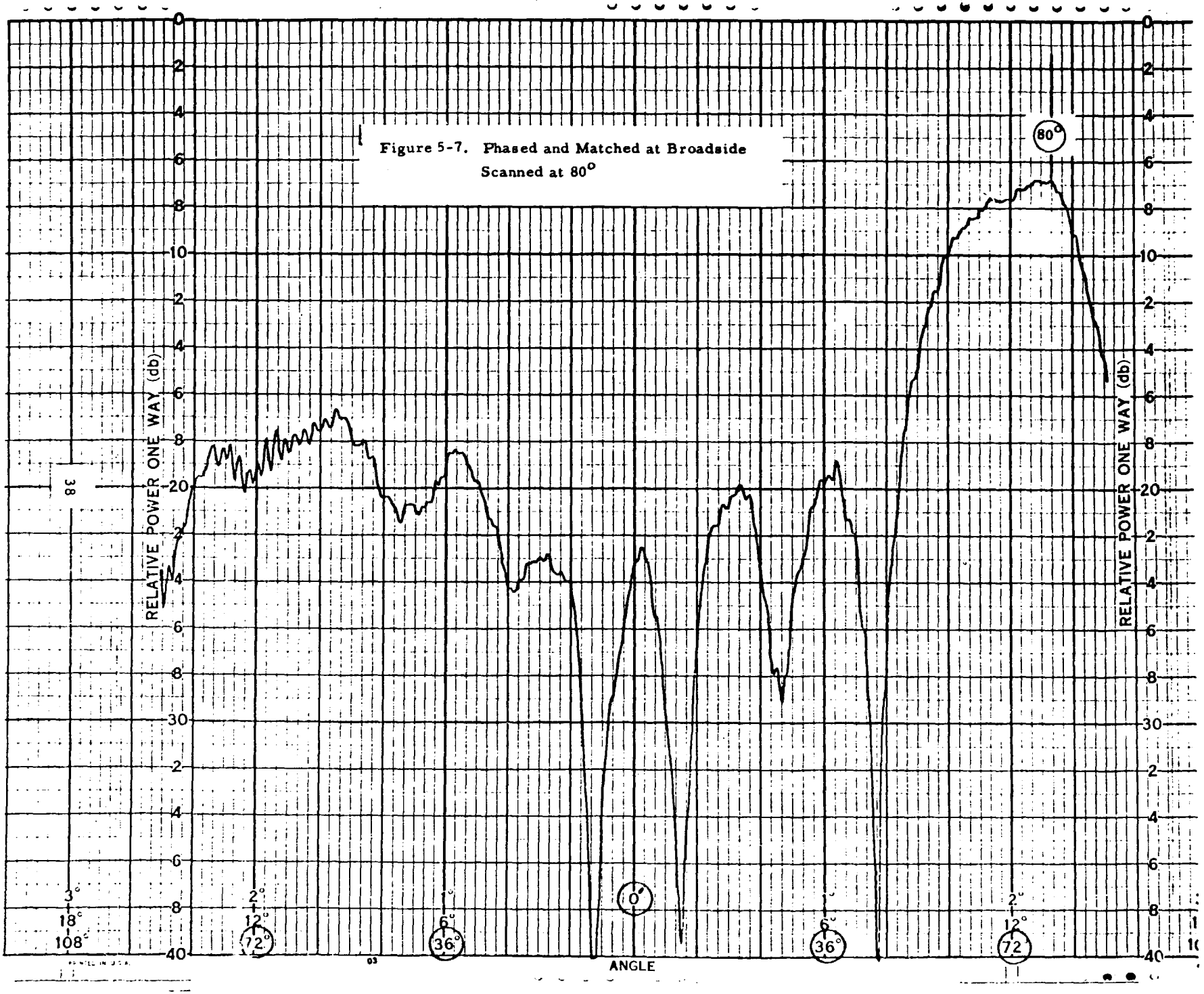

Figure 5-7. Phased and Matched at Broadside Scanned at 80°

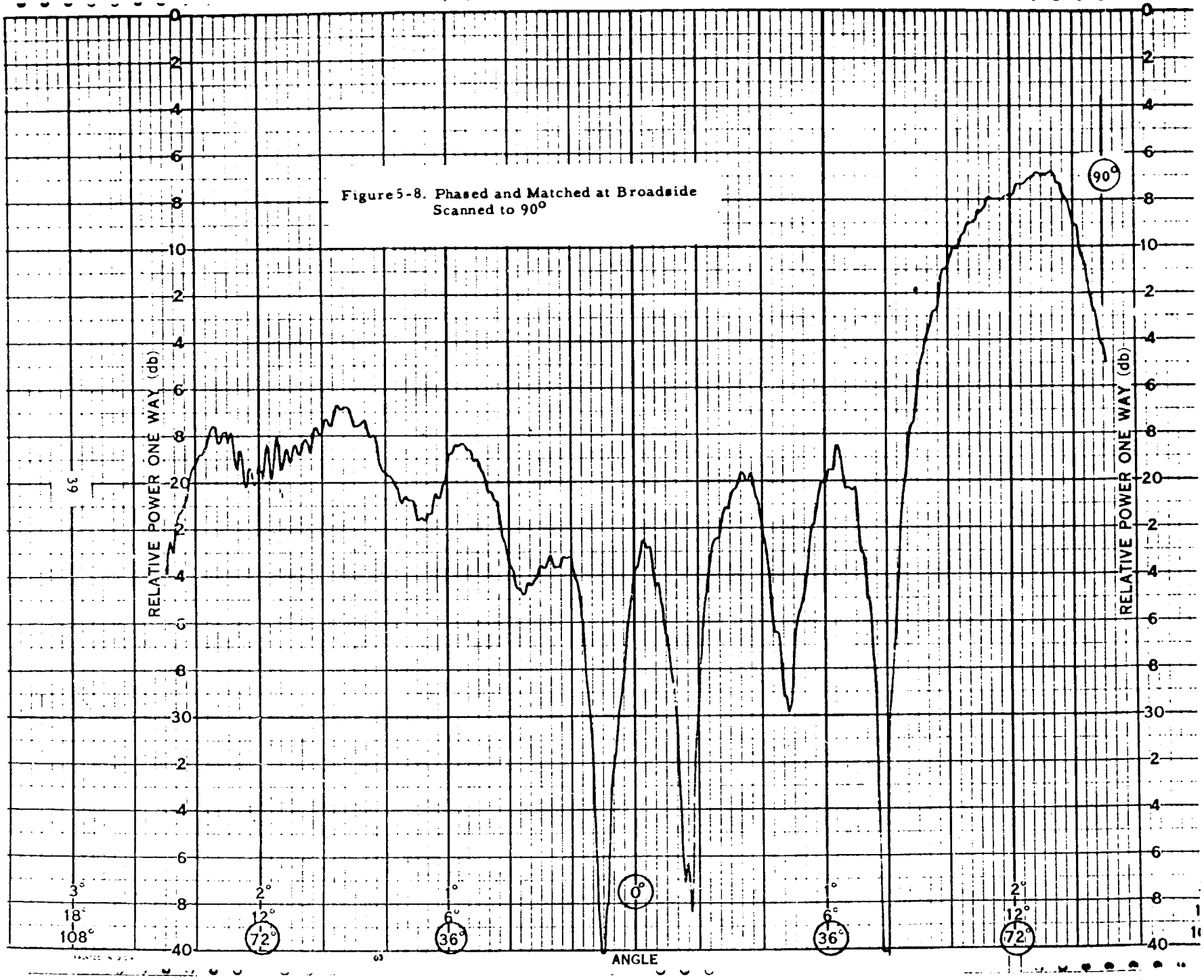

Figure 5-8. Phased and Matched at Broadside Scanned to 90°

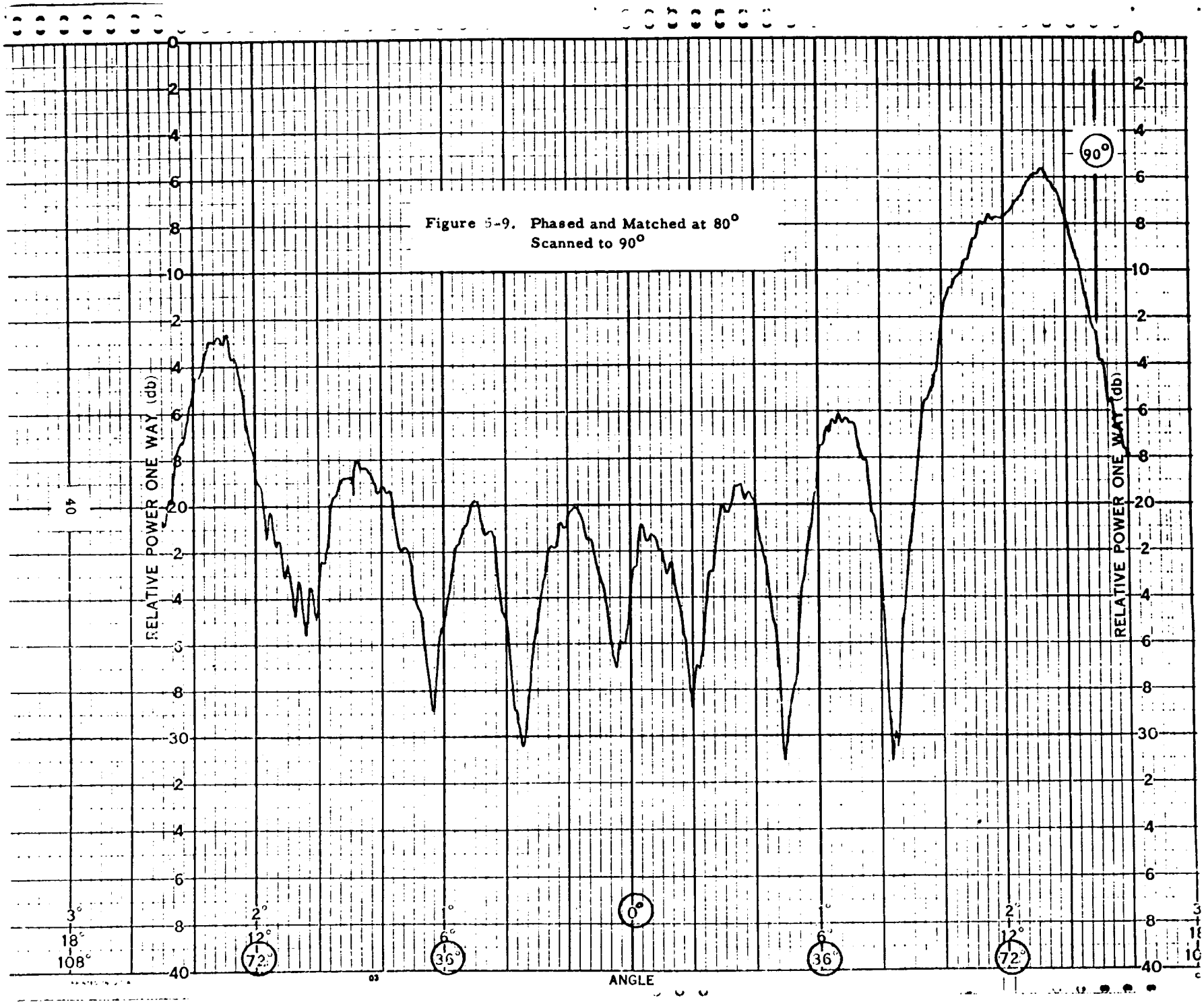

Figure 5-9. Phased and Matched at 80° Scanned to 90°

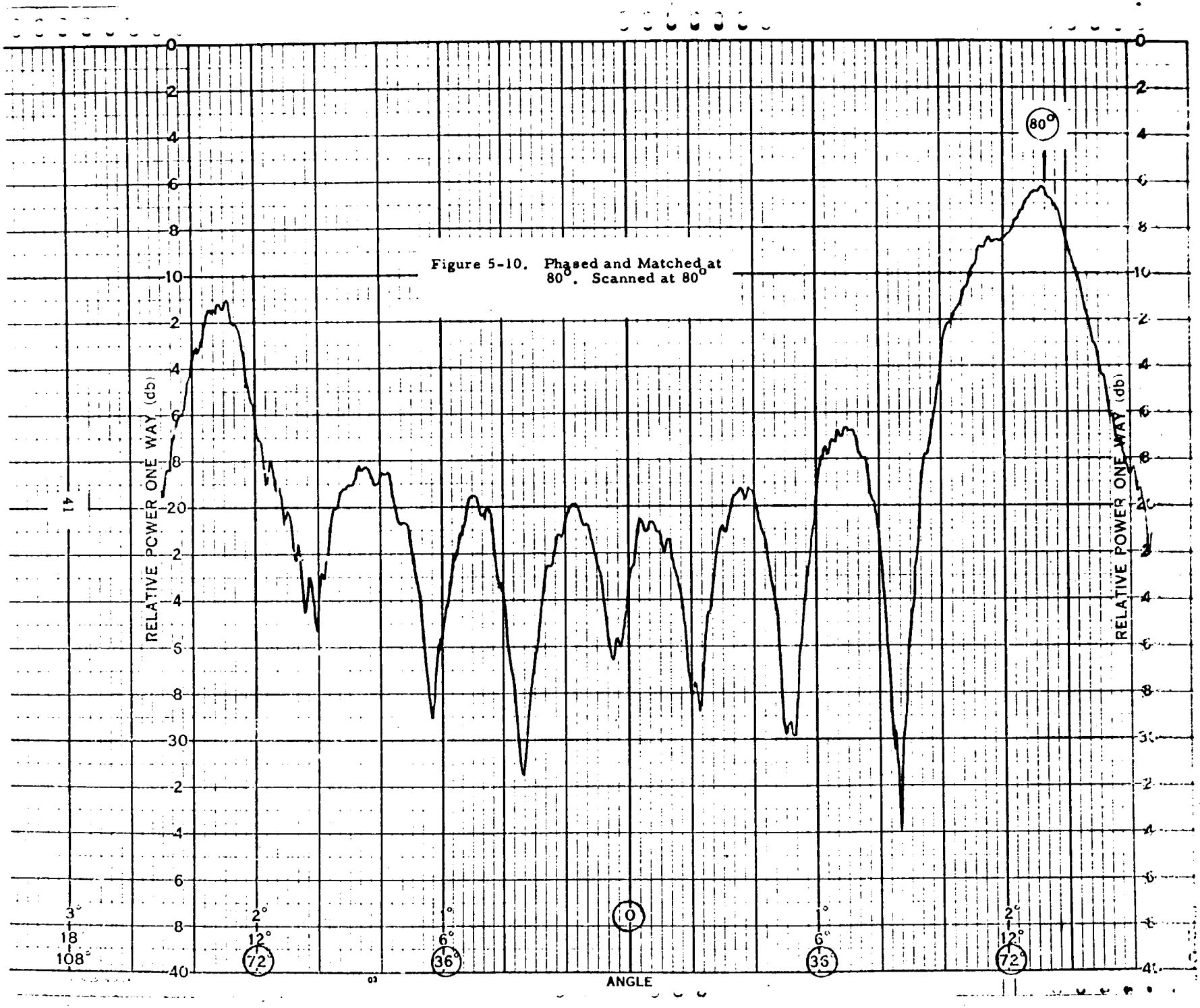

Figure 5-10. Phased and Matched at 80°. Scanned at 80°

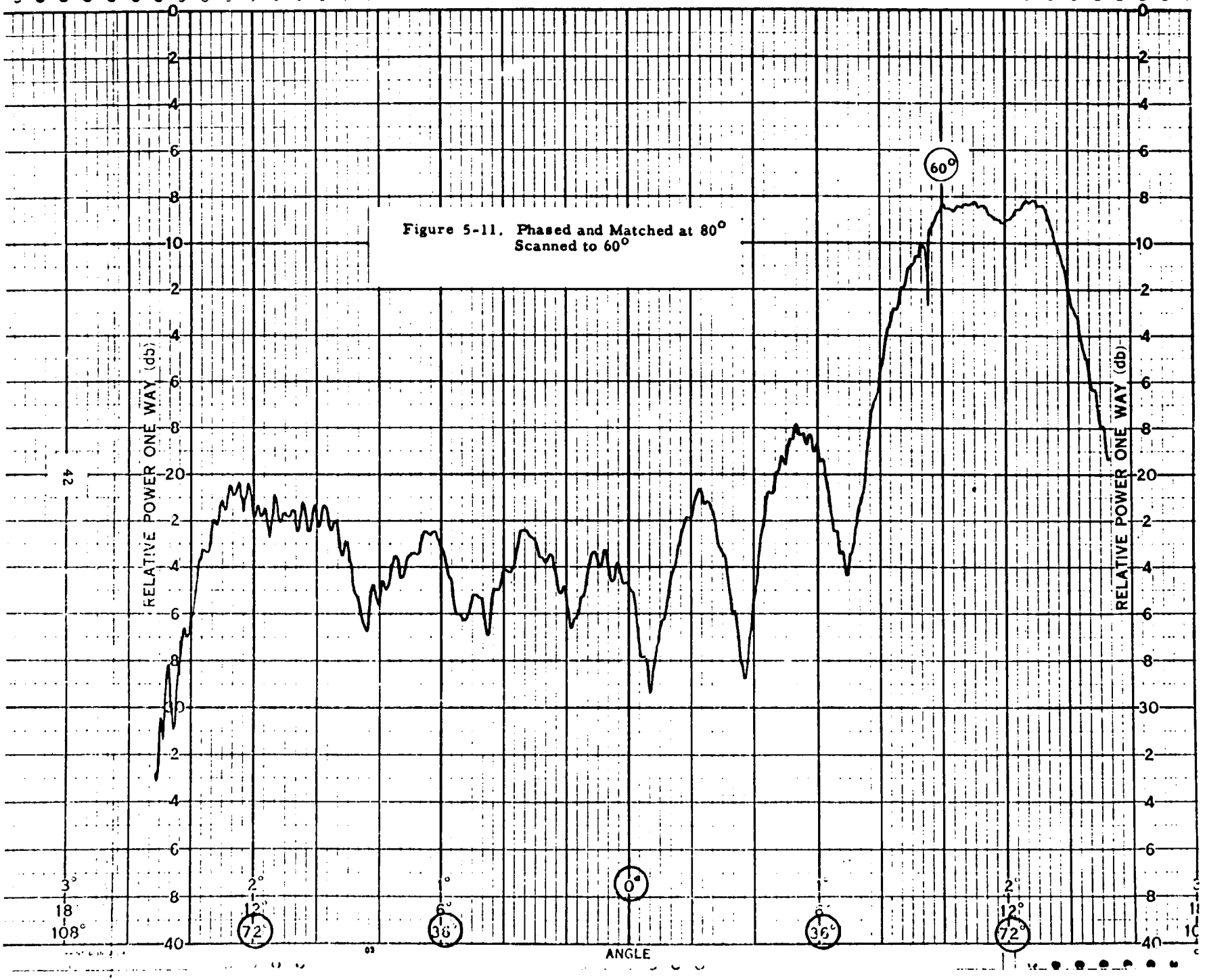

Figure 5-11. Phased and Matched at 80° Scanned to 60°

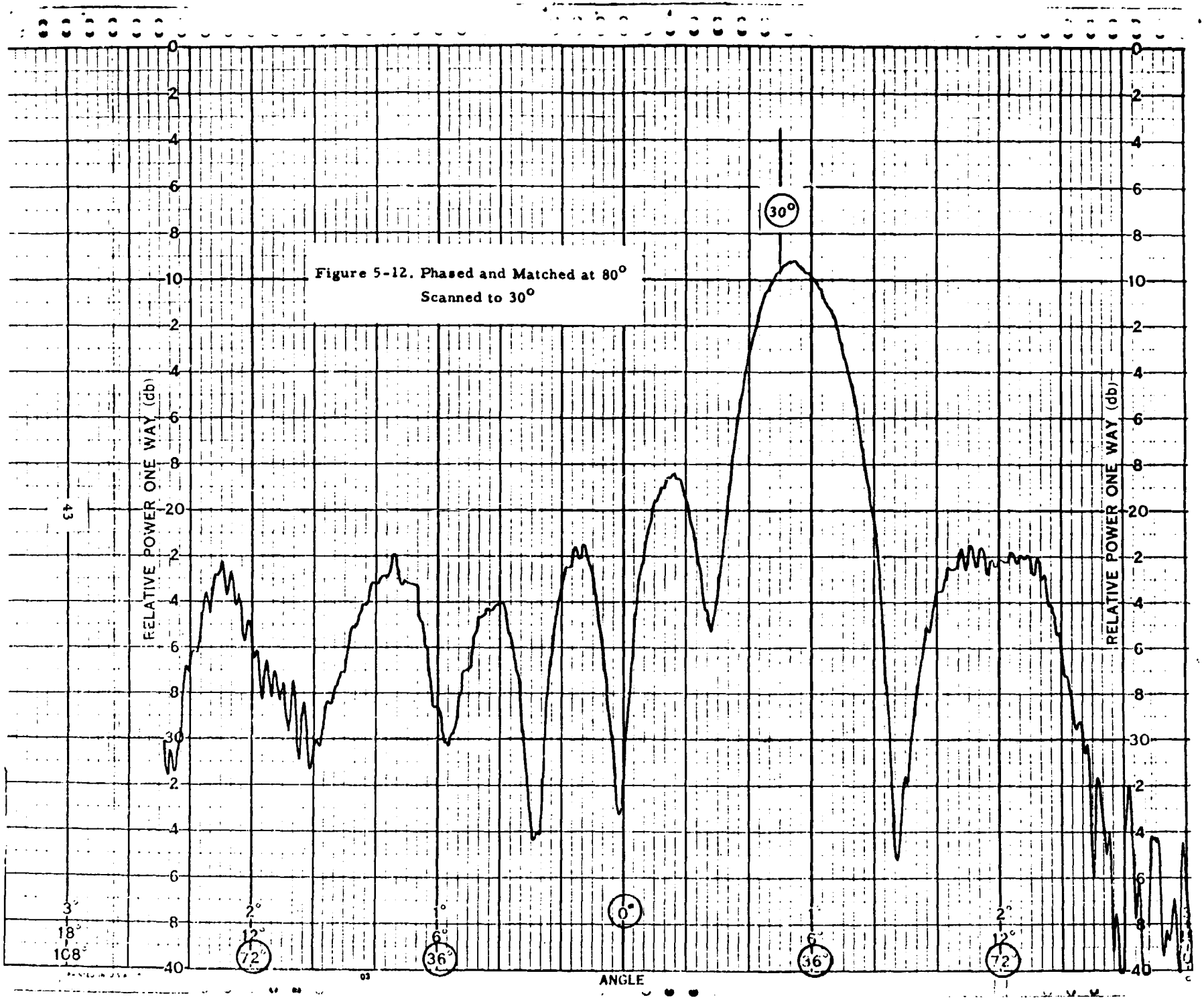

Figure 5-12. Phased and Matched at 80° Scanned to 30°

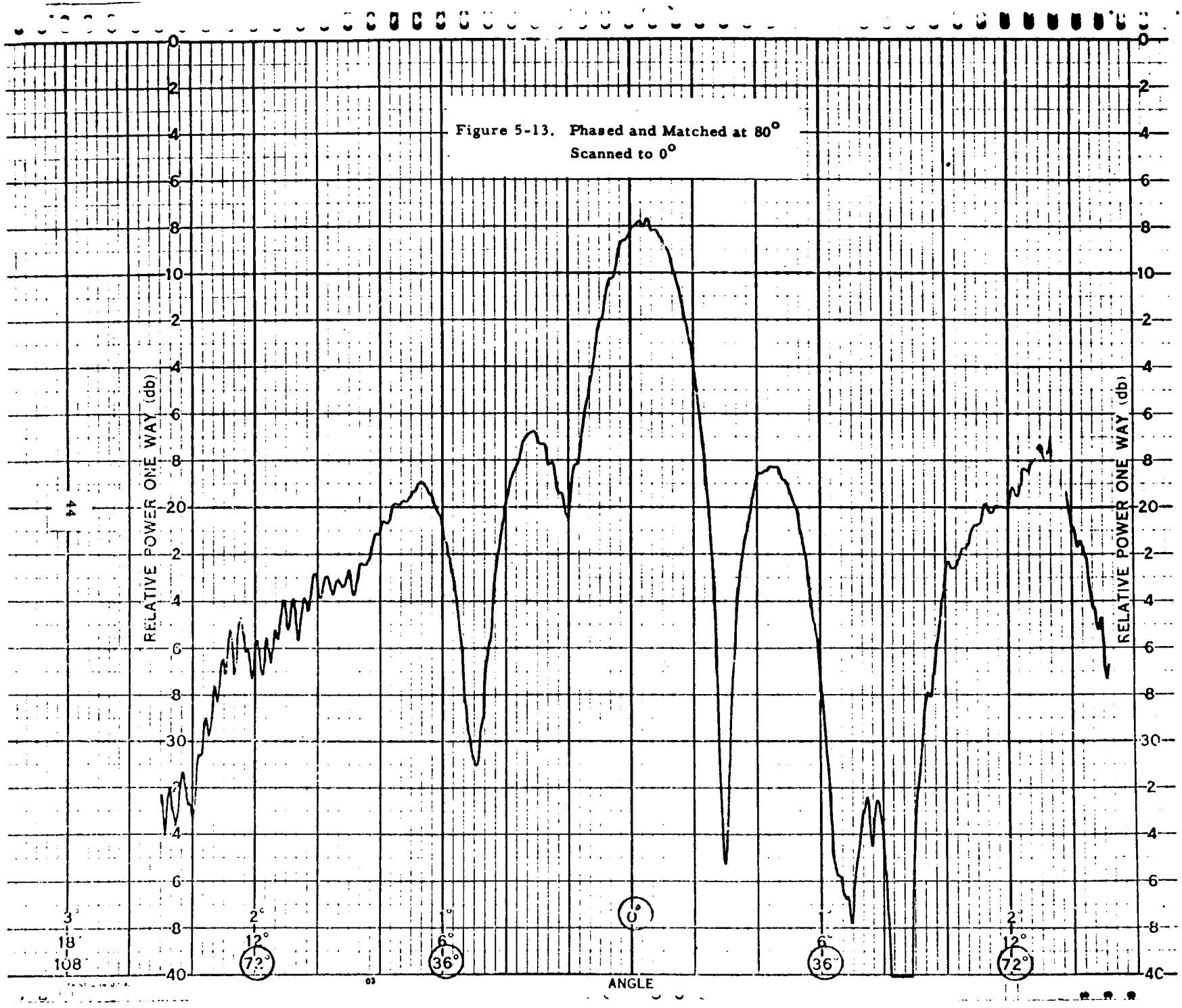

Figure 5-13. Phased and Matched at 80° Scanned to 0°

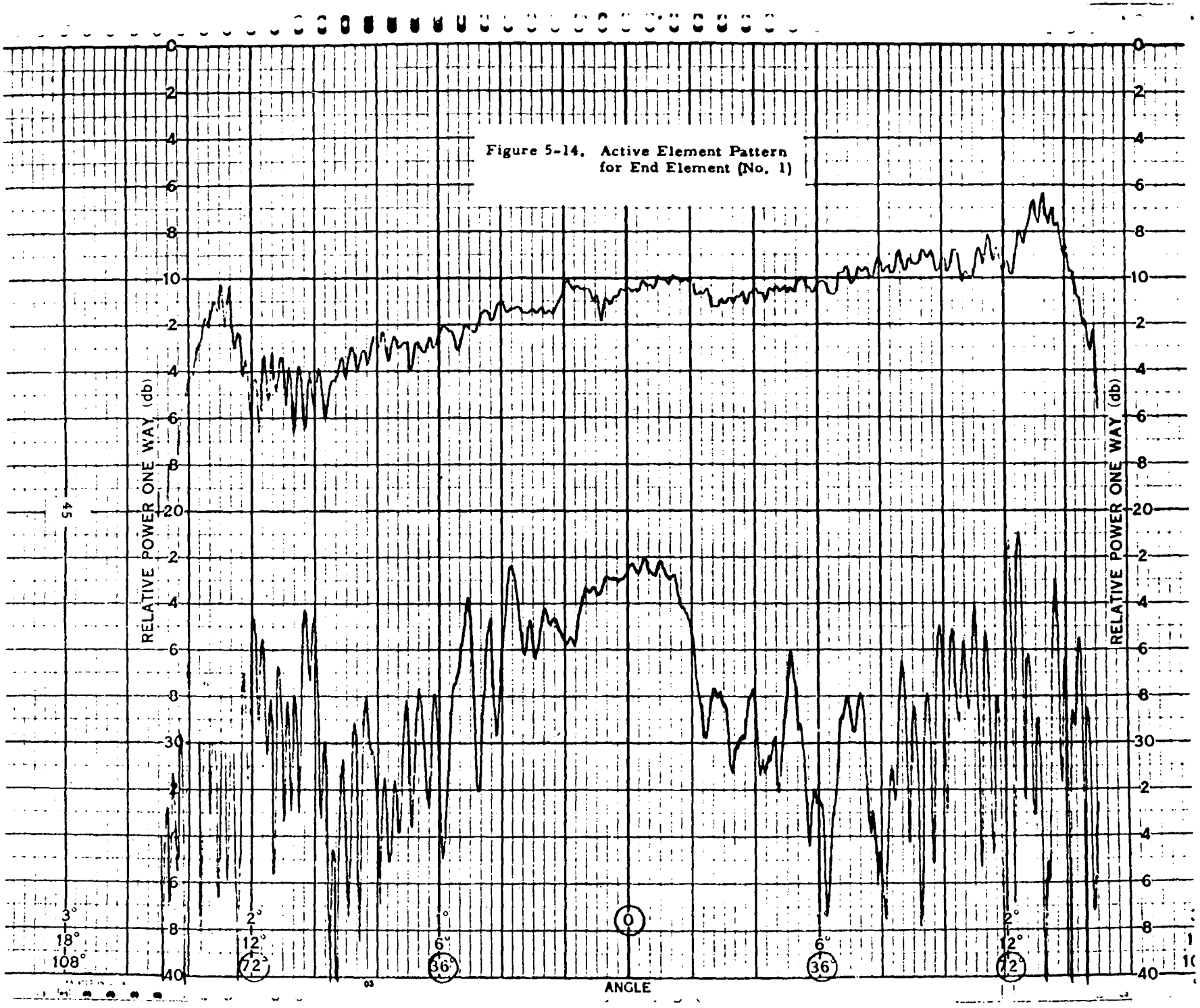

Figure 5-14. Active Element Pattern for End Element (No. 1)

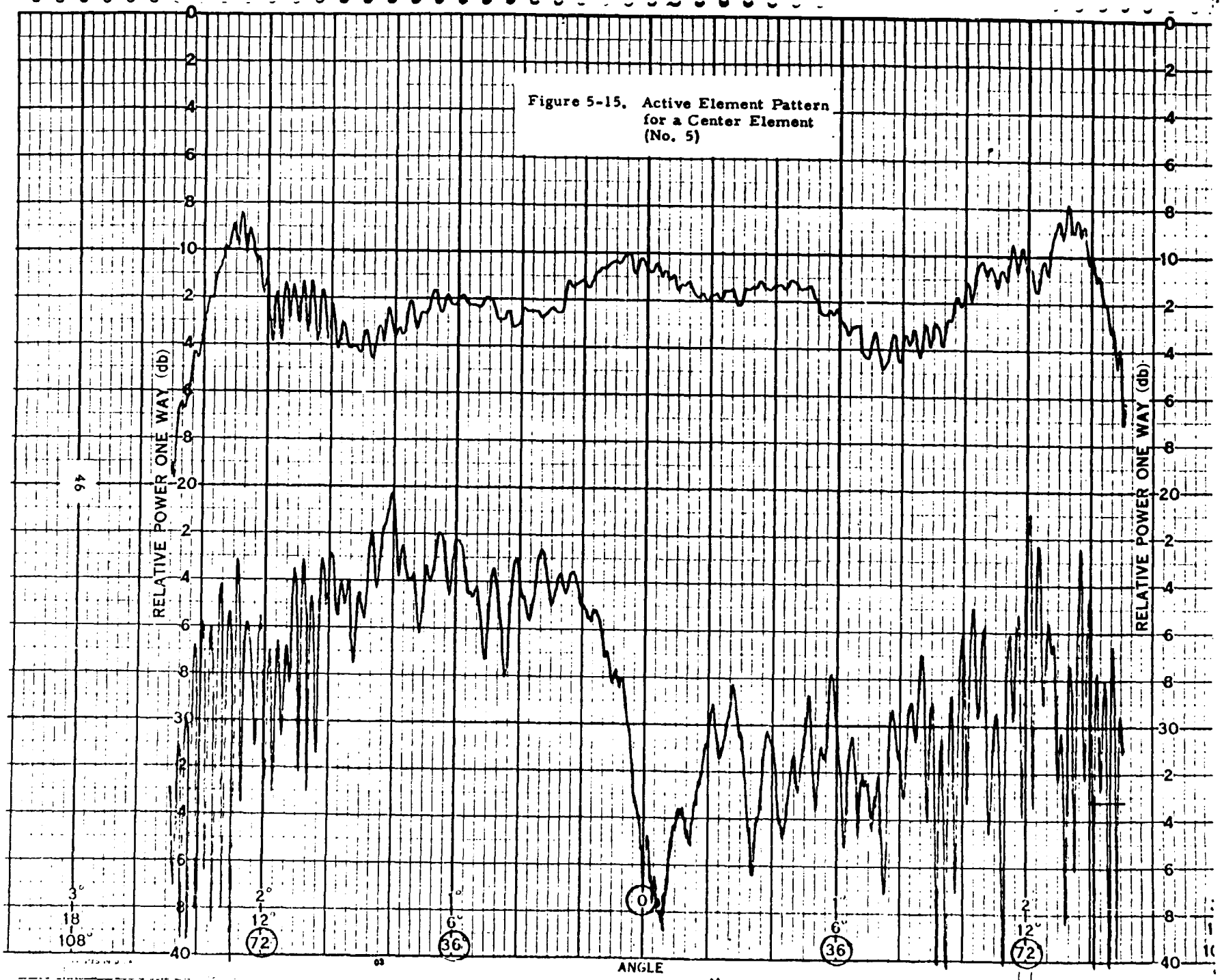

Figure 5-15. Active Element Pattern for a Center Element (No. 5)

The next step will be to compare the active impedances of the elements with those calculated theoretically (Kummer, et al, 1970).

This array will then be incorporated into the model of the previously fabricated metallic cone. The array will be oriented along a generatrix. The scanning capabilities for this type of geometry will be investigated and evaluated.

APPENDIX I

Computer Program for the Computation of the Zeros of the Associated Legendre Functions

The program that has been developed for the computation of the zeros of the Associated Legendre Function of the first kind is listed in this appendix. Certain results obtained from this program checked very well with Gray's (1953) published results for zeroth order (the only order covered in that paper). This program is capable of computing the eigenvalues associated with higher orders, when θ_o is in the neighborhood of π. It thus satisfies the requirements for computing patterns of the conformal array.

```
C   THIS PROGRAM COMPUTES THE ZEROS OF THE ASSOCIATED LEGENDRE
C   FUNCTIONS OF THE FIRST KIND W.R.T. THE DEGREE,COS(THETA) NEAR -1
      DOUBLE PRECISION STEP,Z,Z2,S,RJ,RN,DEL,X,PI,X3,RL1,V,S9,G
      DOUBLE PRECISION RM,RL2,SS1,SS2,SS3,W1,W2,SUM
      DOUBLE PRECISION V2,V3,V4,V5,AJ,RL6,AM,T,T9
      DOUBLE PRECISION P,Q
      DIMENSION P(5130),Q(5130),G(144),S(144),B(16,80)
C   TO AVOID INDETERMINATE FORM 0/0, THE INITIAL PT. WAS SELECTED
C   AS DEL=1/128
C   STEP=SIZE OF INTERVAL FOR WHICH THE FUNCTIONS ARE COMPUTED
C   LOOPS 3,5,7 ARE FOR THE FUNCTION PSI
C   THE FIRST 74 CARDS COMPUTE THE FUNCTION IN (0,2) IN STEP 1/64
      DEL=.0078125
      STEP=.015625
      DO 3 J=1,64
      RJ=J-1
      Z=20.+DEL+STEP*RJ
      Z2=Z**2
      S(J)=DLOG(Z)-1./(2.*Z)-1./(12.*Z2)+1./(120.*Z **2)-1./(252.*Z2**3)
    3 S(J)=S(J)+1./(240.*Z2**4)
      DO 5 J=1,64
      RJ=J-1
      Z=DEL+STEP*RJ
      SUM=0.
      DO 4 N=1,19
      RN=N
    4 SUM=SUM+1./(RN+Z)
    5 S(J)=S(J)-SUM
      DO 7 J=65,129
      RJ=J-65
      Z=1.+DEL+STEP*RJ
    7 S(J)=S(J-64)+1./Z
      SS3=DLOG(20.)-1./40.-1./(12.*400.)+1./(120.*2 .**4)
      SS3=SS3-1./(252.*20.**6)+1./(240.*20.**8)
      SUM=0.
      DO 8 N=1,19
      RN=N
    8 SUM=SUM+1./RN
      SS3=SS3-SUM
      PI=3.14159265358979
C   X IS PI - THETA IN DEGREES OR HALF-ANGLE OF CONE
      X=10.
      X3=(X/2.)*PI/180.
      Z=DSIN(X3)**2
      RL1=DLOG(Z)
C   LOOP 10 IS FOR P(COS(X))
      DO 10 J=1,129
      RJ=J-1
      V=DEL+STEP*RJ
      S9=1.0
      G=1.0
      DO 12 M=1,15
      RM=M
      G=G*(V-RM+1.)*(V+RM)/(RM**2)
   12 S9=S9+G*(-Z)**M
   10 P(J)=S9
      S9=SS3
      DO 333 M=1,15
```

```
      RM=M
      S9=S9+1./RM
  333 Q(M)=S9
C     Q(M) REPRESENTS PSI(M)
C     LOOP 15 IS FOR P(COS(THETA))
      DO 15 J=1,129
      RJ=J-1
      V=DEL+STEP*RJ
      RL2=DSIN(PI*V)/PI
      SS1=S(J)
      SS2=SS1
      SUM=SS1+SS2-2.*SS3
      G=1.
      DO 14 M=1,15
      RM=M
      G=G*(V-RM+1.)*(V+RM)/(RM**2)
      W1=V+RM
      W2=V-RM+1.
      SS1=SS1+1./W1
      SS2=SS2-1./W2
   14 SUM=SUM+G*(SS1+SS2-2.*Q(M))*(-Z)**RM
   15 P(J)=SUM*RL2+P(J)*(RL2*RL1+DCOS(V*PI))
      T=-DCOS(X*PI/180.)
      DO 18 J=1,5000
      RJ=J-1
      V=1.+DEL+STEP*RJ
   18 P(J+128)=((2.*V+1.)*T*P(J+64)-V*P(J))/(V+1.)
      DO 20 M=2,16
      MM=M-1
      DO 19 L=1,MM
   19 B(M,L)=L-1
   20 CONTINUE
C     LOOP 40 COMPUTES THE ROOTS USING LINEAR INTERPOLATION.
C     MM=THE ORDER AND LL=THE L-TH ROOT OF ORDER MM
      DO 40 M=1,16
      MM=M-1
      WRITE (6,902) MM
  902 FORMAT(///2HM=,1I10//)
      RM=M-1
      V6=0.
      IF(M.EQ.1)KK=1
      IF(M.GE.2)KK=(M-1)*64
      LL=M-1
      WRITE(6,910)
  910 FORMAT(///15X,9HM N ROOTS//)
      DO 24 J=KK,5119
      RJ=J-1
      IF(P(J)*P(J+1))25,25,24
   25 V=DEL+STEP*RJ
      LL=LL+1
      IF(P(J).GE.0.)V3=P(J)
      IF(P(J).LT.0.)V3=-P(J)
      IF(P(J+1).GE.0.)V4=P(J+1)
      IF(P(J+1).LT.0.)V4=-P(J+1)
      V5=V+STEP*V3/(V3+V4)
      V7=V5-V6
      B(M,LL)=V5
      V6=V5
```

```
      WRITE (6,903)V5,V7
  903 FORMAT (10X,2F20.8)
   24 CONTINUE
      II=M*64
      JJ=(M-1)*64
      LIMIT=5120-II
      V=1.-DEL+RM
      T9=((2.*V+1.)*T*P(II)-(V-RM+1.)*P(II+64))/(V+RM)
      Q(II)=(V-RM)*T*P(II)-(V+RM)*T9
      DO 27 J=1,LIMIT
      RJ=J-1
      V=DEL+STEP*RJ+RM+1.
      JA=J+JJ
      JB=J+II
   27 Q(JB)=(V-RM)*T*P(JB)-(V+RM)*P(JA)
      LLL=LIMIT+1
      DO 29 J=1,LLL
      L=J-1
      KK=L+II
   29 P(KK)=Q(KK)/4.
   40 CONTINUE
      DO 51 M=1,16
      DO 52 L=1,75
      MM=M-1
   52 WRITE(6,907) MM,L,B(M,L)
  907 FORMAT (5X,2I10,1F20.10)
   51 CONTINUE
 1000 STOP
      END
```

APPENDIX II

Computer Program for the Computation of the Zeros of the Derivative of the Associated Legendre Functions

The program listed in this appendix is similar to the one listed in Appendix I but computes the zeros of the derivative of the associated Legendre Function of the first kind instead of the zeros of the function. Selected results of this program were also checked against published data. They agreed well with the results of Carrus and Treuenfels (1950) for the derivative of the zeroth order (the only order covered in their tables). This program is capable of computing the eigenvalues for the derivative associated with higher orders when θ_o is in the neighborhood of π; and, hence, also satisfies the requirements of the conformal array program.

```
C    THIS PROGRAM COMPUTES THE ZEROS OF THE DERIVATIVE OF THE
C    ASSOCIATED LEGENDRE FUNCTIONS OF THE FIRST KIND W.R.T. THE DEGREE
C    FOR COS(THETA) NEAR -1
       DIMENSION G(144),S(144),P(5130),Q(5130),C(16,80)
       DOUBLE PRECISION V2,V3,V4,V5,AJ,RL6,AM,T,T9
       DOUBLE PRECISION RM,RL2,SS1,SS2,SS3,W1,W2,SUM
       DOUBLE PRECISION STEP,Z,Z2,S,RJ,RN,DEL,X,PI,X3,RL1,V,S9,G
       DOUBLE PRECISION P,Q
C    TO AVOID INDETERMINATE FORM 0/0, THE INITIAL PT. WAS SELECTED
C    AS DEL=1/128
C    STEP=SIZE OF INTERVAL FOR WHICH THE FUNCTIONS ARE COMPUTED
C    LOOPS 3,5,7 ARE FOR THE FUNCTION PSI
C    THE FIRST 74 CARDS COMPUTE THE FUNCTION IN (0,2) IN STEP 1/64
       DEL=.0078125
       STEP=.015625
       DO 3 J=1,64
       RJ=J-1
       Z=20.+DEL+STEP*RJ
       Z2=Z**2
       S(J)=DLOG(Z)-1./(2.*Z)-1./(12.*Z2)+1./(120.*Z2**2)-1./(252.*Z2**3)
     3 S(J)=S(J)+1./(240.*Z2**4)
       DO 5 J=1,64
       RJ=J-1
       Z=DEL+STEP*RJ
       SUM=0.
       DO 4 N=1,19
       RN=N
     4 SUM=SUM+1./(RN+Z)
     5 S(J)=S(J)-SUM
       DO 7 J=65,129
       RJ=J-65
       Z=1.+DEL+STEP*RJ
     7 S(J)=S(J-64)+1./Z
       SS3=DLOG(20.)-1./40.-1./(12.*400.)+1./(120.*20.**4)
       SS3=SS3-1./(252.*20.**6)+1./(240.*20.**8)
       SUM=0.
       DO 8 N=1,19
       RN=N
     8 SUM=SUM+1./RN
       SS3=SS3-SUM
       PI=3.14159265358979
C    X IS PI - THETA IN DEGREES OR HALF-ANGLE OF CONE
       X=10.
       X3=(X/2.)*PI/180.
       Z=DSIN(X3)**2
       RL1=DLOG(Z)
C    LOOP 10 IS FOR P(COS(X))
       DO 10 J=1,129
       RJ=J-1
       V=DEL+STEP*RJ
       S9=1.0
       G=1.0
       DO 12 M=1,15
       RM=M
       G=G*(V-RM+1.)*(V+RM)/(RM**2)
    12 S9=S9+G*(-Z)**M
    10 P(J)=S9
       S9=SS3
```

```
      DO 333 M=1,15
      RM=M
      S9=S9+1./RM
  333 Q(M)=S9
C   Q(M) REPRESENTS PSI(M)
C   LOOP 15 IS FOR P(COS(THETA))
      DO 15 J=1,129
      RJ=J-1
      V=DEL+STEP*RJ
      RL2=DSIN(PI*V)/PI
      SS1=S(J)
      SS2=SS1
      SUM=SS1+SS2-2.*SS3
      G=1.
      DO 14 M=1,15
      RM=M
      G=G*(V-RM+1.)*(V+RM)/(RM**2)
      W1=V+RM
      W2=V-RM+1.
      SS1=SS1+1./W1
      SS2=SS2-1./W2
   14 SUM=SUM+G*(SS1+SS2-2.*Q(M))*(-Z)**RM
   15 P(J)=SUM*RL2+P(J)*(RL2*RL1+DCOS(V*PI))
      T=-DCOS(X*PI/180.)
      DO 18 J=1,5000
      RJ=J-1
      V=1.+DEL+STEP*RJ
   18 P(J+128)=((2.*V+1.)*T*P(J+64)-V*P(J))/(V+1.)
C   LOOP 80 COMPUTES THE ROOTS USING LINEAR INTERPOLATION.
C   MM=THE ORDER AND LL=THE L-TH ROOT OF ORDER MM
      DO 80 M=1,16
      MM=M-1
      RM=MM
      LL=0
      V6=0.
      WR+TE(6,911) MM
  911 FO-MAT (///5X,2HM=1I5//)
      DO 60 J=1,5064
      RJ=J-1
      V=DEL+STEP*RJ
   60 Q(J)=(V-RM+1.)*P(J+64)-(V+1.)*T*P(J)
      DO 64 J=1,5063
      RJ=J-1
      IF (Q(J)*Q(J+1)) 63,63,64
   63 V=DEL+STEP*RJ
      LL=LL+1
      IF (Q(J).GE.0.) V3=Q(J)
      IF (Q(J).LT.0.) V3=-Q(J)
      IF (Q(J+1).GE.0.) V4=Q(J+1)
      IF (Q(J+1).LT.0.) V4=-Q(J+1)
      V5=V+STEP*V3/(V3+V4)
      V7=V5-V6
      C(M,LL)=V5
      V6=V5
      WRITE (6,903) V5,V7
  903 FORMAT (10X,2F20.8)
   64 CONTINUE
      DO 66 J=1,5128
```

```
      RJ=J-1
      V=DEL+STEP*RJ
      IF(J.GE.5064)Q(J)=(V-RM)*T*P(J)-(V+RM)*P(J-64)
      IF(J.LT.5064)Q(J)=(V-RM+1.)*P(J+64)-(V+RM+1.)*T*P(J)
   66 CONTINUE
      DO 67 J=1,5128
   67 P(J)=Q(J)/4.
   80 CONTINUE
      DO 70 M=1,16
      DO 71 LL=1,75
      MM=M-1
      WRITE (6,907) MM,LL,C(M,LL)
  907 FORMAT (5X,2I10,1F20.10)
   71 CONTINUE
   70 CONTINUE
      DO 72 J=1,5128,25
      RJ=J-1
      V=DEL+STEP*RJ
   72 WRITE (6,913) V,P(J),P(J+5),P(J+10),P(J+15),P(J+20)
  913 FORMAT (5X,1F10.6,5E12.4)
 1000 STOP
      END
```

REFERENCES

Bailin, L. L. and S. Silver (1956). "Exterior Electromagnetic Boundary Value Problems for Spheres and Cones," IRE T-AP, AP-4, pp. 5-16, January, 1956. Correction IRE T-AP, AP-5, p. 313, July, 1957.

Carrus, P. A. and C. C. Treuenfels (1950), "Tables of Roots and Incomplete Integrals of Associated Legendre Functions of Fractional Orders," J. Math. Physics., 29, pp. 282-299.

Gray, M. C. (1953). "Legendre Functions of Fractional Order," Quart. of App. Math., 11, pp. 311-318, October, 1953.

Kummer, W. H., A. T. Villeneuve, J. E. Howard, A. F. Seaton, (1970). "Integrated Conformal Arrays, Final Report, pp. 77-86; March, 1970, Contract N00019-69-C-0281, Hughes Aircraft Company.

Villeneuve, A. T. and J. E. Howard (1968). "Integrated Conformal Arrays, pp. 31-34, Contract N00019-68-C-2014, Section 4, May-August, 1968, Hughes Aircraft Company

Unclassified

Security Classification

DOCUMENT CONTROL DATA - R & D

(Security classification of title, body of abstract and indexing annotation must be entered when the overall report is classified)

1. ORIGINATING ACTIVITY (Corporate author)	2a. REPORT SECURITY CLASSIFICATION
Hughes Aircraft Company Culver City, California	Unclassified
	2b. GROUP

3. REPORT TITLE

INTEGRATED CONFORMAL ARRAYS (U)

4. DESCRIPTIVE NOTES (Type of report and inclusive dates)

Final Report March 1970 to January 1971

5. AUTHOR(S) (First name, middle initial, last name)

Wolfgang H. Kummer
Marvin C. Behnke
Alfred T. Villeneuve
Arthur F. Seaton

6. REPORT DATE	7a. TOTAL NO. OF PAGES	7b. NO. OF REFS
February 15, 1971	62	5

8a. CONTRACT OR GRANT NO.	9a. ORIGINATOR'S REPORT NUMBER(S)
N00019-70-C-0397	2765.01/266 HAC Ref. No. C-1498
b. PROJECT NO.	
c.	9b. OTHER REPORT NO(S) (Any other numbers that may be assigned this report)
d.	

10. DISTRIBUTION STATEMENT

DISTRIBUTION LIMITED TO U.S. GOVERNMENT AGENCIES ONLY;

☐ FOREIGN INFORMATION
☐ PROPRIETARY INFORMATION
☐ TEST AND EVALUATION
☐ CONTRACTOR PERFORMANCE EVALUATION

Contractor Imposed Distribution Statement

DATE: April 1971

OTHER REQUESTS FOR THIS DOCUMENT MUST BE REFERRED TO COMMANDER, NAVAL AIR SYSTEMS COMMAND, AIR-310B

11. SUPPLEMENTARY NOTES

12. SPONSORING MILITARY ACTIVITY

Naval Air Systems Command
Department of Navy
Washington, D. C.

13. ABSTRACT

Two distinct aspects were investigated in this program. The first one is concerned with the synthesis of far field patterns from sources on the conical surface. Three different approaches were undertaken:

(1) An equivalence principle was used to determine the distribution of sources on a cone to produce a prescribed pattern in the far field.

(2) Roots of two transcendental equations were calculated for appropriate parameters. The numerical values are needed for a theoretical solution of the radiation fields and mutual coupling effects in a region bounded by a conducting cone.

(3) Computation of patterns from discrete radiators placed on a conical surface was continued. The signal-to-noise ratio is optimized in the beam pointing direction.

The second aspect included the design, fabrication and testing the scanning capabilities of a linear array of crossed slots on a large ground plane. The array was designed so that each radiating element could be matched in the presence of the others, its phase and amplitude could be arbitrarily set and the active impedance measured. The array scanned from broadside to 80° (10° from endfire) with satisfactory beam patterns and sidelobe levels.

DD FORM 1 NOV 65 1473

Unclassified

Security Classification

KEY WORDS	LINK A		LINK B		LINK C	
	ROLE	WT	ROLE	WT	ROLE	WT